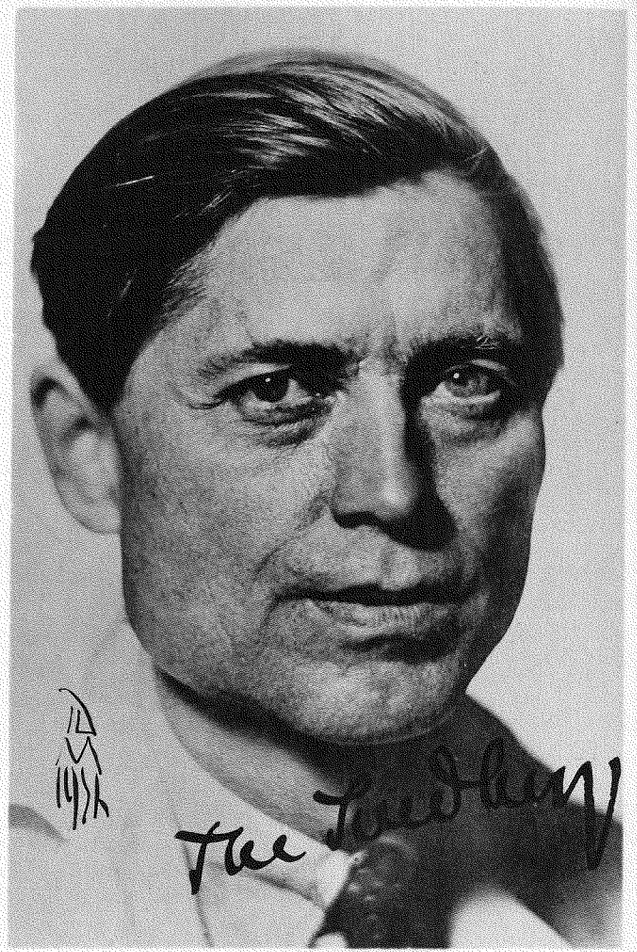

THE SVEDBERG, 1884 –

ANNALS OF THE NEW YORK ACADEMY OF SCIENCES
VOLUME XLIII, ART. 5. PAGES 173–252
OCTOBER 6, 1942

THE ULTRACENTRIFUGE*

BY

D. A. MACINNES, W. J. ARCHIBALD, J. W. BEAMS, W. B. BRIDGMAN, ALEXANDRE ROTHEN, AND J. W. WILLIAMS

CONTENTS

*This series of papers is the result of a conference on the Ultracentrifuge held by the Section of Physics and Chemistry of the New York Academy of Sciences, November 14 and 15, 1941. Manuscript received by the editor, May 1942.

Publication made possible through a grant from the income of the Conference Publications Revolving Fund.

INTRODUCTION TO THE CONFERENCE ON THE ULTRACENTRIFUGE

By D. A. MacInnes

From the Laboratories of The Rockefeller Institute for Medical Research, New York

One of the most powerful methods for studying proteins, and other substances of high molecular weight, is the ultracentrifuge. As a matter of fact it was that instrument, as developed by The Svedberg, which first showed that proteins have definite molecular weights. Since Svedberg's pioneering work the ultracentrifuge has proved to be an important aid in biological investigations, because, in addition to indicating the molecular weights of large molecules, it can separate the substances present in a mixture of proteins into groups according to their molecular masses, and, in certain cases, effect actual separations.

Although the ultracentrifuge is now a most useful tool its development is far from complete, in either its experimental or theoretical aspects, as the papers that follow clearly show. In the near future the precision of the data obtained will be increased by closer regulation of temperature, of speeds of rotation, and by improved optical systems. The interpretation of the resulting data will in certain cases be facilitated by utilization of the more elaborate theory, already at hand, of the instrument.

In addition to a discussion of the whole field, the chairman had two main ideas in arranging the conference. The first was that of seeing whether the theoretical developments of Archibald, which he outlines in a paper given below, could not be put to practical use. As is well known, the ultracentrifuge is utilized in two different ways: (1) in the determinations of sedimentation rates; and (2) in the measurements of the equilibrium distributions. The first of these has the advantage of the rapidity with which measurements can be made, but requires diffusion measurements if the results are to be interpreted in terms of molecular weights. The second method requires careful regulation of the speed and temperature over long periods of time, but requires no additional data for the interpretation of the data. The theories for these limiting cases are relatively simple. But there is a series of states, as the equilibrium condition is being approached, the data on which might be interpreted in terms of the more complex theory, if that theory could be made available to the experimentalist. This could be done by putting the results in tabular or graphical form. We have been encouraged to believe that government aid will eventually be available for

this project. Such tables and graphs will be particularly useful in studying the smaller proteins and other materials of relatively low molecular weight.

Another matter which the chairman wished to have discussed was that of adopting zero degrees centigrade as the standard temperature for the measurement of physical properties of proteins and solutions of proteins. There are at least two good reasons for such a standard temperature. Proteins gain in stability as the temperature is decreased. Also electrophoretic measurements are made at, or near, zero degrees. If values of sedimentation constants, viscosity, diffusion constants, etc., all were obtained at that temperature it would eliminate the present necessity of considering temperature coefficients, with the attendant uncertainties.

The members of the conference, which included most, if not all, of the active workers in the field in the United States, indicated a desire to honor Professor The Svedberg, to whose pioneering experiments the ultracentrifuge is due. It was unanimously decided: first, to dedicate the monograph resulting from the proceedings of the conference to Professor Svedberg; and second, to adopt, as a convenient practical unit for sedimentation constants, the *Svedberg*, to be denoted by the letter S and equal to 10^{-13} times the absolute units, which are in seconds. This seems particularly fitting since S is the initial letter both of Professor Svedberg's name, and of the unit of time in which sedimentation constants are expressed.

THE PRODUCTION AND MAINTENANCE OF HIGH CENTRIFUGAL FIELDS FOR USE IN BIOLOGY AND MEDICINE

By J. W. Beams

From the Rouss Physical Laboratory, University of Virginia, Charlottesville

Many of the effects of centrifugal force undoubtedly were known in ancient times because it comes into action whenever a moving body changes its direction of motion. In fact, it occurs so often, and its effects are so pronounced, that one almost subconsciously allows for it in his everyday activities. Probably it is for this reason that, early in the period when the foundations of our present theory of mechanics were being laid, the quantitative relation connecting centrifugal force with the other known properties of a body and its motion were worked out.

The purpose of this paper is to review briefly some of the recent work in the production and maintenance of high centrifugal fields which may be of use for medical and biological research. The value of high centrifugal fields in such researches results principally from the fact that substances either in suspension or solution will settle out when subjected to sufficiently high centrifugal fields. Or, if they are in the solid state, stresses are set up by the centrifugal field which oppose the forces holding them together. In 1847 Stokes showed that the velocity of fall, v, of a spherical particle of density, d_p, and radius, a, in a liquid of density, d_e, and coefficient of viscosity, η, in a gravitational or centrifugal field, F, is given by the equation:

$$v = \frac{2}{9\eta} (d_p - d_e)\, a^2\, F. \qquad (1)$$

From this relation of Stokes it will be observed that the rate of settling of a particle is doubled if its density is doubled or increased four-fold if its radius is doubled, its density remaining the same. It is, therefore, evident that the process of settling or sedimentation in a gravitational or centrifugal field separates particles of different sizes and different densities. It is, of course, a common observation that such is the case. In fact, the process of settling in the gravitational field of the earth or in a comparatively low speed centrifuge is used widely as a means of separating particles of different sizes and densities in mining and manufacturing processes. On the other hand, it is also a common observation that this will occur only when the particles are uncharged and com-

paratively large, for when the radius of the particle approaches that of molecular dimensions, sedimentation in appreciable amounts no longer takes place; *i.e.*, an unsaturated sugar or salt solution may be left to stand or may be centrifuged in a low speed centrifuge for many years without settling out of solution. The reason for this apparent failure of Stokes' law for particles with radii of molecular dimensions arises from the fact that the rate of sedimentation is opposed by the rate of diffusion. Diffusion arises from the thermal agitation or Brownian motion of the particles and always operates to transport particles from regions of high concentration to regions of low concentration, which is in just the direction to oppose sedimentation. According to the well known theory[1] in the case of uncharged molecules, of molecular weight M, the sedimentation in a centrifuge will proceed until the concentrations c_1 and c_2 at distances r_1 and r_2 from the axis of rotation reaches the values given by the relation:

$$\log_e \frac{c_1}{c_2} = \frac{M\ (1 - Vd)\ w^2\ (r_1^2 - r_2^2)}{2\ RT}, \tag{2}$$

where d is the density of the solvent, V the partial specific volume, T the absolute temperature, R the gas constant, and w is the angular velocity or $2\pi n$, where n is the number of revolutions per second. If each particle occupies a volume, V, the sedimentation will proceed until:

$$\log_e \frac{c_1}{c_2} = \frac{NV\ (d_p - d_e)\ w^2\ (r_1^2 - r_2^2)}{2\ RT}, \tag{3}$$

where N is the Avogadro number. It will be observed from the above relations that the ratio of the concentrations, c_1/c_2, which is a measure of the maximum sedimentation obtainable, increases very rapidly both with M and w for a given centrifuge. In the modern high speed centrifuge wr, which equals the peripheral velocity, v, is large enough to produce a sizable concentration change between the center and the periphery of the centrifuge for substances with molecular weights as low as that of sugar or common salt and, in the case of the heavy protein molecules of molecular weights 10^4 or greater, the concentration change is almost infinite. Consequently, the high speed centrifuge is a practical means of measuring particle or molecular weights, as every term in equation (2) other than M can be measured. As pointed out, equation (2) is an expression for the equilibrium case where sedimentation is balanced by diffusion. Weaver[2] and Archibald[3] have shown theoretically, and

[1] **Svedberg, T.** "Colloid Chemistry," 2d edit., Chemical Catalog Co., Inc. New York. 1928; Nature. **139:** 1051. 1937; Proc. Roy. Soc., Series B. **127:** 1. 1939.
[2] **Weaver, W.** Phys. Rev. **27:** 499. 1926.
[3] **Archibald, W. J.** Phys. Rev. **53:** 746. 1938; **54:** 371. 1938.

Svedberg[4] and others have demonstrated experimentally, that the time required for this equilibrium to be attained is in general very long. Consequently, in practice in the high speed centrifuge for the heavier molecules not only does c_1/c_2 become too large to measure with precision but it also requires too long a centrifuging time. This centrifuging time is of the order of several days in some cases. Fortunately, as Svedberg[1] early pointed out, when M is large (as in the case of many proteins) the velocity of sedimentation of the molecules in a high speed centrifuge is large enough to be measured directly. In such cases the velocity of sedimentation dr/dt is given by the expression:

$$\frac{dr}{dt} = \frac{M\ (1 - Vd)}{f}\ w^2 r = \frac{M\ (1 - Vd)\ D\ w^2 r}{RT}, \tag{4}$$

where r is the distance from the axis, D is the diffusion constant and f is the friction constant. Methods of measuring dr/dt in a centrifuge are to be discussed later in this program, and it will suffice for our present purpose to point out that for the most powerful centrifuges dr/dt should be as large as possible. In practice the *rate of sedimentation* method of equation (4) supplements the *equilibrium* method of equation (2), so that in designing a high speed centrifuge both methods must be kept in mind.

Essentially, the two methods require different rotor designs because w^2r^2 or the (peripheral velocity)^2 multiplies the mass, M, in equation (2), whereas w^2r or the centrifugal force multiplies M in equation (4). In other words, for the equilibrium method one must design for as large a peripheral velocity as possible, while for the rate of sedimentation method one designs for as large a centrifugal force as possible. This, of course, is true only in a general way because, as we shall see, for some purposes the absolute value of the centrifugal force must be sacrificed to avoid too great a variation in the centrifugal force, etc.

At the present time the factor which limits both maximum centrifugal force and the maximum peripheral velocity attainable is the bursting strength of the rotor. For rotors of similar shape which are not loaded, theory shows that in general the bursting speed is determined by the peripheral velocity of the rotor squared (w^2r^2). Consequently, other things being equal, the size of the rotor for use with the equilibrium method is not important; *i.e.*, large rotors will give as large a peripheral velocity as small ones so that one can pick a rotor size convenient for other purposes. On the other hand, the smaller the diameter of a rotor of a given shape, the larger is the centrifugal force (w^2r) that can be produced. Therefore, for the rate of sedimentation method, other

[4] **Svedberg, T., & Pedersen, K. O.** The Ultracentrifuge." Clarendon Press. Oxford. 1940.

things being equal, the rotor diameter should be as small as possible. Although these rules for an unloaded rotor serve as general guides for proper design, many other factors must be considered. The rotor must always carry a load and, if this load is a liquid whose boundaries are at distances r_1 and r_2 from the axis of rotation, the pressure developed is given by: $P = \frac{dw^2}{2}[r_1^2 - r_2^2]$, where d is the density of the liquid. Hence, for minimum pressure the rotor should have as small a radius as possible. On the other hand, when the liquid to be centrifuged is contained in a tight centrifuge cell mounted on the rotor, it is the centrifugal force times the mass that produces the rotor stress. As will be seen later, a rotor of given radius, in order to reach a maximum rotational speed without bursting, must be so shaped that local stresses do not reach the yield point of the rotor material. Ideally, the stresses throughout the rotor should be almost uniform at maximum rotor speed. In practice, this is never attained but in order to approach it each rotor must be designed for its particular use.

If the maximum separation in a centrifuge is to be obtained, in addition to high centrifugal forces, remixing or stirring due to convection currents in the material being centrifuged must be eliminated. Remixing arises principally from accelerations, decelerations or vibrations of the centrifuge, and from temperature gradients in the centrifuge cell. The first three are comparatively easy to prevent by proper design, but elimination of the last requires the greatest care. One can best visualize how temperature gradients produce convection in a centrifuge cell by remembering that convection currents will take place in a vessel of water if the lower part is slightly warmer than the upper part. The principal force which produces these convection currents is proportional to the product of the difference in densities (produced by an unequal temperature between the top and bottom of the vessel), and the force of gravity. If the centrifugal force is many hundred thousand times gravity, as is the case in a high speed centrifuge, clearly the temperature must be uniform or it must vary in such a way as to make the density increase toward the periphery. Actually, when the temperature throughout the cell is uniform, the density increases toward the periphery because of the increase in pressure. But this is comparatively small, so that in practice the temperature must be very uniform. Svedberg and his collaborators[4] have shown that to obtain convection-free sedimentation the centrifuge cell should be sector shaped because this allows all of the particles to follow the direction of the force. On the other hand, when the centrifuge is used as a means of purifying materials, a certain type

of convection may be an advantage and often is deliberately introduced.[5–7] The angular type of centrifuge is a good example of this, but a discussion of convection at this time would take us too far afield.

The technique of driving high speed centrifuges has been developed practically within the last decade and a half. In 1924 Svedberg and his associates set a record by producing a centrifugal field of 5000 times gravity in a convection free centrifuge cell, and today the use of fields of several hundred thousand times gravity is routine for many investigators using several different types of machines. In general, the most satisfactory types of high speed centrifuges are driven electrically or by means of liquids or gases. The ordinary belt and gear drives which are so successful for low speed rotors have not proven very satisfactory for rotational speeds above 800 to 1000 r.p.s.

SVEDBERG CENTRIFUGE

The Svedberg oil driven ultracentrifuge[4] is designed to give centrifugal force in the range from 15,000 to 750,000 g, or as high as the rotor will spin without exploding. The rotor is of a special nickel steel alloy and designed with the view of preventing stresses in one region of the loaded rotor from rising too far above those in the other parts. It is supported in horizontal bearings and driven by twin oil turbines on each end of the rigid shaft. The cell which contains the material to be centrifuged is provided with crystal quartz windows for observing the sedimentation. Surrounding the rotor is a thermostated heavy close fitting steel case. The turbines are driven by oil supplied by a special compressor, which is filtered and brought to the proper temperature before striking the turbines. Special ingenious oil dampers are provided in the bearings to damp out vibrations in the rotor and its rigid shaft induced by the oil impinging on the turbines, friction on the rotor, critical vibrations, etc. Hydrogen at about 20 mm. pressure is continuously circulated through the rotor chamber. Hydrogen at this pressure has a large ratio of heat conductivity to rotor friction and thus helps to maintain uniform temperature throughout the centrifuge cell. The rotor containing the cell and its contents is carefully balanced both statically and dynamically before the machine is operated.

These oil turbine ultracentrifuges of Svedberg are the result of excellent machine design and most careful workmanship. They have been used primarily for analytical work by Svedberg and his associates in

[5] **Bauer, J. H., & Pickels, E. G.** Jour. Exp. Med. **64**: 503. 1936; **65**: 565. 1937; **71**: 703. 1940.
[6] **Wyckoff, R. W. G.** Proc. Am. Phil. Soc. **77**: 455. 1937; Science **86**: 92, 311, 1937; Jour. Biol. Chem. **121**: 219. 1937; **122**: 239. 1937; **124**: 585. 1938.
[7] **Masket, A. V.** Rev. Sci. Instr. **12**: 277. 1941.

their epoch-making studies of protein molecules. An excellent description of this machine is given in a recent book by Svedberg and Pedersen[4] to which reference is made for further details.

GAS DRIVEN CENTRIFUGES

There are two types of high speed air driven centrifuges which are in comparatively wide use. The first type spins in air at atmospheric pressure. Although it had been known for a long time that rotors could be supported and spun by air, Henriot and Huguenard[8] in 1925 first succeeded in spinning small rotors to ultra high speeds (11.7 mm. rotor to 11,000 r.p.s.). This method of Henriot and Huguenard has been modified and improved by a number of different workers[9,10] until at the present time it is most useful. FIGURE 1 shows a sketch of an apparatus

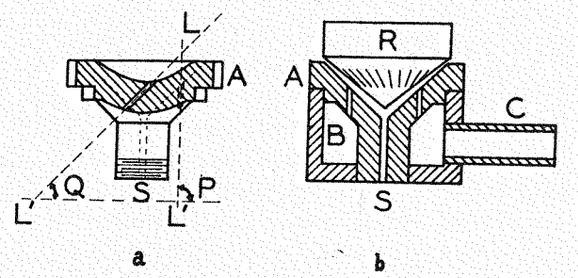

FIGURE 1. Diagram of air-driven, air-supported centrifuge: (a) on central section through stator cone; (b) section through complete machine.

which has been used successfully in our laboratory for about ten years. It consists of a stator cone, *A*, an air box, *B*, and a cone-shaped rotor, *R*. The stator cone and air box can be made of any machinable material, but the rotor should be made of alloy steel or Duralumin ST 14. Compressed air which enters the air box *B* through *C* emerges through the tubes *LL'* in jets. These jets impinge upon the flutings of the rotor, lift it off the stator, and start it spinning. The cone-shaped surfaces of the rotor and stator are shaped so that the Bernouilli forces prevent the rotor from flying out of the stator and constrain it to spin on a thin cushion of air. The channel, *S*, allows air to flow into the stator from the atmosphere and stabilize the supporting air film. This air cushion

[8] **Henriot, E., & Huguenard, E.** Compt. Rend. **180**: 1389. 1925; Jour. Phys. et Rad. **8**: 433. 1927.
[9] **Beams, J. W.** Rev. Sci. Instr. **1**: 667. 1930; Jour. App. Phys. **8**: 795. 1937; Rev. Mod. Phys. **10**: 245. 1938; in "Science in Progress." G. A. Baitsell, ed. Series 2. Yale University Press. New Haven, Conn. 1940. pp. 232–264.
[10] **McBain, J. W.** Chem. Rev. **24**: 289. 1939.

"bearing" is not only very stable but allows the rotor to "seek its own axis of rotation." In practice, these properties are a great advantage because they avoid the necessity of accurate dynamical balancing of the rotor, and allow the rotor to be loaded or unloaded while at full speed. Also, the so-called "center of flotation" may be well below the center of gravity of the rotor so that the rotor can carry a considerable superstructure.

FIGURE 2 shows the relation between rotor speed and driving air pressure for typical rotors. Curves *A*, *B*, *C*, and *D* are for a 1⅛″ rotor carrying superstructures of various sizes. It is clear that the air friction at atmospheric pressure is very large at high surface speeds. For this reason, unless a large volume of air at high pressure is used, rotors more than a few inches in diameter cannot be spun at high speeds. But with smaller rotors high centrifugal fields can be produced. The maximum speed for a gas-driven rotor that has been obtained in our laboratory was with a 9 mm. rotor driven by hydrogen. It reached a speed of almost a million and a half revolutions per minute and produced a centrifugal field of almost eight million times gravity.

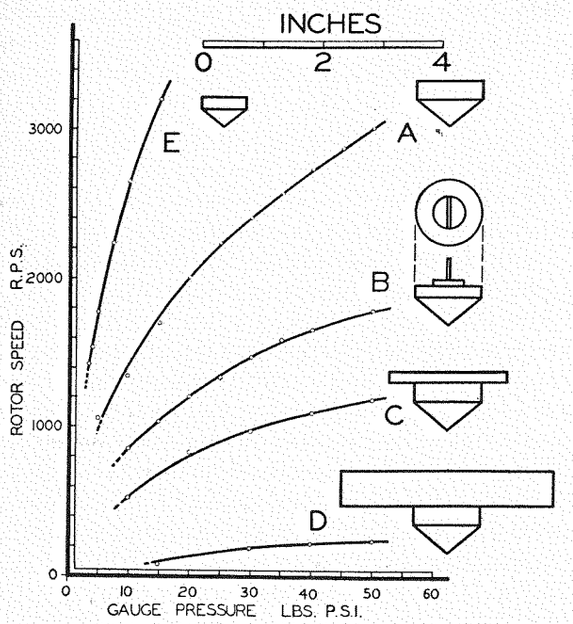

FIGURE 2. Relation between rotor speed and driving air pressure for rotors shown at right of curves.

Unfortunately, the expanding air jets which impinge upon the under surface of the rotor cool it while the air friction around the periphery and above, heat those parts, so that temperature gradients exist in the rotor. These gradients, although not great, are large enough to produce remixing unless care is taken in the design to prevent it. Several investigators have used such rotors successfully in molecular sedimentation studies. In experiments in which precise temperature control is not essential and in which a large centrifugal field is necessary over only a small radial distance, this machine is almost ideal. For example, Beams and King[11], Harvey[12], and many others have used this type of machine in most interesting studies of sedimentation inside a biological cell. If the specimen to be centrifuged is small, so that it can be maintained at uniform temperature, this type of centrifuge is especially useful. Also, it can be recommended for sedimentation studies when precise results are not required. The required materials cost but a few dollars and the construction requires only a few hours of an instrument maker's time. It can be recommended as a handy, inexpensive tool to have in the laboratory if air pressure is available.

THE VACUUM-TYPE OF AIR-DRIVEN CENTRIFUGE

In the vacuum-type of centrifuge the rotor spins in a vacuum on a flexible vertical shaft. It thus completely avoids the troublesome effects of air friction and obviates extreme precision in the dynamical balance of the rotor. Even in the early crude air-driven vacuum-type machines which Pickels and I[13] first constructed, the sedimentation was convection-free and the centrifugal force was limited only by the bursting speed of the rotor. The various present designs of these machines differ somewhat, but essentially they consist of a large centrifuge rotor located inside a vacuum-tight chamber; a smaller, air-driven, air-supported turbine situated above or below the chamber; and a small, thin, flexible shaft which fastens them together and which is co-axial with their common axis of rotation. FIGURE 3 shows a section of an air-driven vacuum-type centrifuge[9] which has proved very satisfactory for the purification of substances of large molecular weight. C is the centrifuge rotor inside the vacuum chamber, V; T is the air-supported air-driven turbine; and A is a flexible steel vertical shaft. G_1 and G_2 are vacuum-tight oil glands mounted in flexible round oil-resistant neoprene rings. Vacuum pump oil (low vapor pressure) is forced into these glands and

[11] **Beams, H. W., & King, R. L.** Anat. Rec. **59**: 363, 395. 1934; Proc. Roy. Soc. Series B. **118**: 264. 1935; Nature **135**: 232. 1935; Biol. Bull. **71**: 188. 1936; **73**: 99. 1937; **75**: 189. 1938.
[12] **Harvey, E. N.** Jour. Frank. Inst. **214**: 1. 1932; Jour. App. Phys. **9**: 68. 1938.
[13] **Beams, J. W., & Pickels, E. G.** Rev. Sci. Instr. **6**: 299. 1935.

serves both to lubricate the bearing and seal the vacuum chamber. The rotating members are supported on an air cushion between B and T and are spun by air from S impinging upon the flutings of T. A similar reverse air drive is provided to decelerate the apparatus. The air cushion provides a support or thrust bearing which has very little friction. The air support requires a pressure from about 10 to 20 lbs./m^2 depending upon the weight of the rotor. For the 6-inch Duralumin rotor shown, the supporting pressure is about 12 lbs./in.^{2} The driving air pressure is about 50 lbs./in.^{2} during the period of acceleration (15 to 20 minutes) and from 10 to 20 lbs./in.^{2} during operation at full speed. For the acceleration of this machine one should have a compressed air supply of 20 cu. ft. of air (N.T.P.) per min. at a pressure of 50 lbs./in.^{2} Several methods have been used to measure the rotational speed, as well as to regulate it, but for most purposes some form of the stroboscopic method is satisfactory.

The principal advantage of the flexible shaft is that it allows the centrifuge rotor to seek its own axis of rotation and thus does not require accurate dynamical balance. This is very important, especially for the angular type of rotor, as C of FIGURE 3. This rotor is bored to take a series of lusteroid test tubes which are filled with the material to be centrifuged. During centrifuging, the heavy fractions collect at the bottom of the tubes and the light fractions at the top.

Incidentally, Masket[7] has improved the quantity type of rotor by changing the design so that each of the tubes in the rotor can be plugged individually as shown in FIGURE 4. This allows each tube to be completely filled, making possible the centrifuging of more liquid at one time. Also the tubes are arranged to make a smaller angle with the vertical which, as shown by Wyckoff[6], greatly increases the efficiency. Masket is able to centrifuge 100 cc. of liquid in a field of almost 300,000 times gravity with a 6-inch rotor.

At maximum speed, if one test tube contains one drop more liquid than the others the unbalancing force is almost 40 lbs. without the flexible shaft. Also the small shaft has reduced bearing friction and hence does not become hot even at the highest speed (if necessary, its temperature may be kept very constant by circulating oil). Furthermore, the flexible shaft with its small clearance in G_1 and G_2 avoids the small wobble (of half the rotational frequency and an amplitude of approximately the bearing clearance) usually present when a stiff shaft spins in a journal bearing. Clearly, if this wobble did exist, it would not be appreciably transmitted by the flexible shaft. The large rotor, C, not only spins smoothly about its "natural" axis of rotation but it is

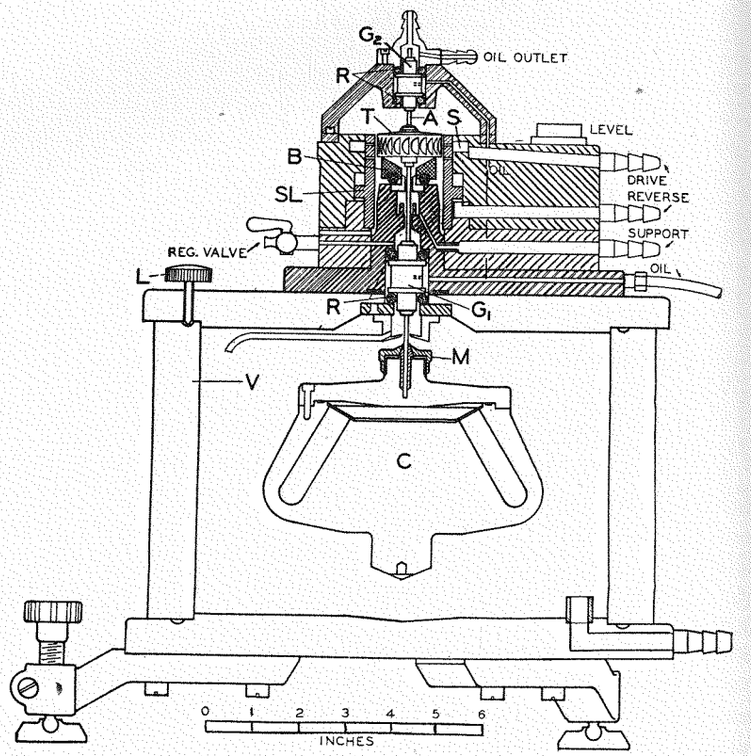

FIGURE 3. Section of air-driven, vacuum-type centrifuge used for concentration of large molecular weight substances.

remarkably free of wobbles and precession and nutation. The damping of these wobbles and precession and nutation is due, in part at least, to the internal friction in the flexible shaft. It might be noted here that a rotor spinning in a vacuum is more stable than when surrounded by air. Kapitza[14] has discussed the effect of air or gaseous friction on a high speed rotor and has shown that it introduces a definite instability in the motion of the rotor. Consequently, the large rotor spinning on a vertical flexible shaft in a vacuum not only avoids all troublesome temperature gradients which arise from air friction, but is free from harmful mechanical wobbles and vibrations. Also the vertical axis avoids a minute ripple of two times gravity in each revolution which, although too small to complicate sedimentation, may act as a power

[14] **Kapitza, P. L.** Jour. Phys. USSR. **1**: 29. 1939.

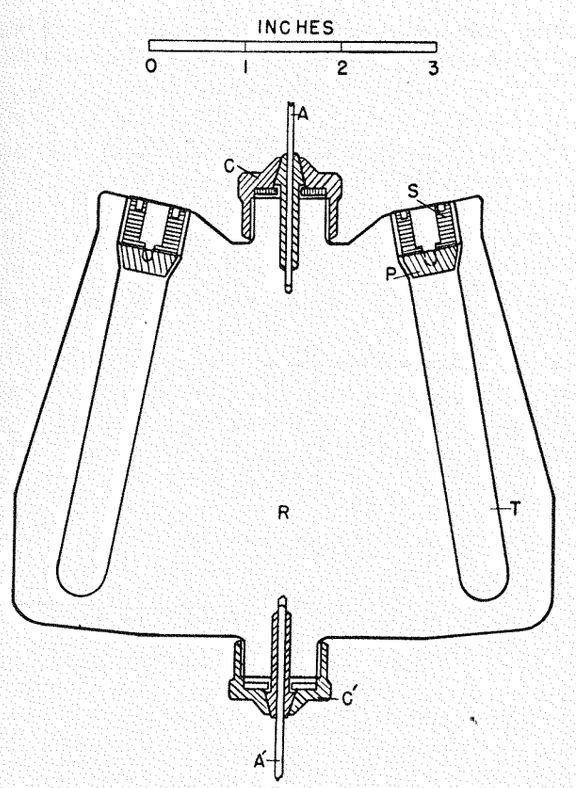

FIGURE 4. Cross section of Masket type of rotor having 102 cc. capacity.

source for generating vibrations. Both of these properties make such a rotor spinning in a vacuum most useful for analytical work (measurement of molecular weights, etc.), especially when optical methods are used to observe the rate of sedimentation. For analytical work with the machine of FIGURE 3 the rotor, *C*, is removed and an analytical rotor with transparent crystal quartz windows is substituted. The sedimentation is observed through windows (not shown in FIGURE 3) in the top and bottom of the vacuum chamber.

As mentioned before, the limiting factor of the centrifugal field attainable is the bursting strength of the rotor. Therefore, attention to rotor design is of utmost importance. The strength of a rotor of a given shape which carries no load is determined by the ratio of the yield strength to the density. Consequently, rotors made of the strong,

light aluminum alloys are almost as good as those made of heat-treated alloy steel. For example, Duralumin ST 14 has a yield point of about 63,000 lbs./in.^{2} and a density of 2.8 and therefore corresponds to a steel which has a yield point of about 180,000 lbs./in.^{2} and a density of 7.82. It is almost impossible to machine a heat-treated alloy steel with a yield point much above 200,000 lbs./in.^{2} Consequently, if a steel stronger than this (and therefore harder) is to be used, it must be heat-treated after machining. This usually warps it out of shape and necessitates difficult grinding operations. We have used for some of our rotors chrome moly steel 4130 X and alloy steel 4340 X, having yield points of about 200,000 lbs./in.^{2}, which can be machined. Svedberg uses a somewhat stronger special nickel alloy steel, but he has found that the strongest hard steels are inferior to the tougher but weaker nickel steels. On the other hand, Duralumin is very easily machined when heat-treated to its maximum strength. Another important advantage of Duralumin, resulting from its smaller density, is its lower kinetic energy of rotation. Obviously, this not only reduces the power required for acceleration but in case of an explosion is far less dangerous. The Duralumin rotors also are easily tested for flaws by X ray. As mentioned previously, the criterion followed in designing a rotor for the highest rotational speed is to shape it so that stresses in one part do not rise appreciably above those in other parts. For this reason, the analytical rotors which carry a centrifuge cell usually have an ellipsoidal shape. Another type of rotor used with the air-driven vacuum-type centrifuge is simply a tube with a solid core. This rotor is used for the type of centrifuge where the material flows into the top of the machine at a continuous rate and out at the bottom as light and heavy fractions.

THE ELECTRICALLY DRIVEN, MAGNETICALLY SUPPORTED VACUUM-TYPE ULTRACENTRIFUGE

Although the air-driven, air-supported, vacuum-type centrifuge just described possesses practically all the desirable features of an ideal centrifuge, it is not completely automatic in operation without auxiliary equipment. Unless the air pressure applied to the turbine is carefully regulated, the rotational speed may vary and eventually explode the rotor if the pressure gets too high. A number of investigators have devised successful ways of regulating the rotor speed, but these are usually somewhat complicated. Also in many laboratories air pressure is not available and an air-compressor must be installed. Clearly it would simplify matters if a centrifuge having all the desirable characteristics

of the air-driven vacuum-type centrifuge, but driven by an electrical motor, could be developed. FIGURE 5 shows a partial section of such a centrifuge which has been in use at Virginia for about two years[15]. The rotating system consists of the steel motor armature, D, the steel magnetic support core, R, the flexible shaft, A, and the duralumin ST 14 rotor, C. The shaft is a hollow tube from G_3 to above G_2 through which cooling water passes. The rotor, C, flexible shaft, A, vacuum chamber, V, and oil glands, G_1 and G_2, are the same as in the air-driven vacuum-type centrifuge described previously. The only differences are that an

[15] **Skarstrom, C., & Beams, J. W.** Rev. Sci. Instr. **11**: 398. 1940.

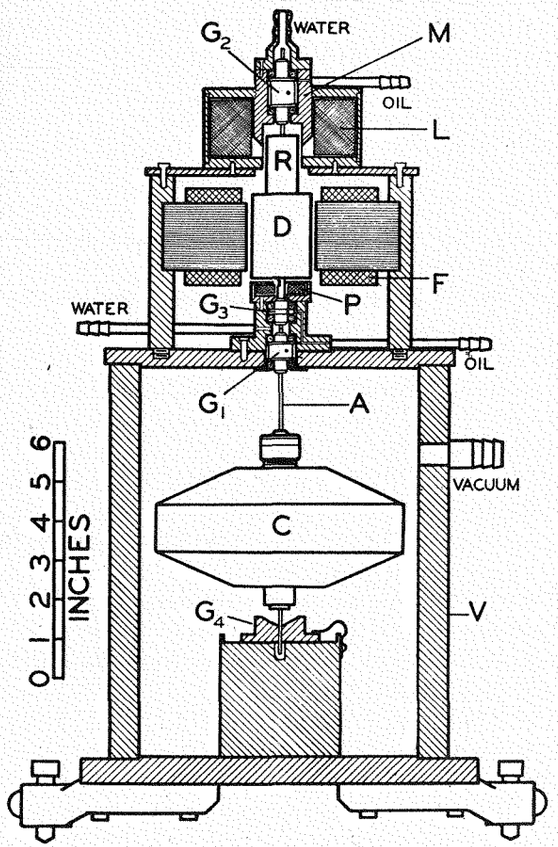

FIGURE 5. Section of magnetically supported, electrically driven, vacuum-type centrifuge.

electrical motor is substituted for the air drive and a magnetic support is used instead of an air support. The small remaining weight is borne by a small thrust bearing consisting of the upper Babbitt surface of G_3 and a small rotating collar on the shaft. This small "oil" thrust bearing is able to support the entire weight of the rotating system in case the power supply of the lifting solenoid should fail. This type of magnetic support is almost friction-free, because the magnetic field of L is symmetrically distributed over the end of R, *i.e.*, there is no electro-magnetic drag.

The four field coils, F, of the motor are supplied with a high-frequency, two-phase alternating current in such a way that the field rotates with the same frequency as the alternating current. The rotating field in F induces currents in the solid steel armature, D, which cause it to rotate. This type of induction motor is well suited to this problem because a comparatively large torque on the armature is produced when the difference between the rotor speed and the frequency of the alternating current is large. As a result, the desired fixed alternating current frequency can be applied to the motor and the armature will start from rest and accelerate to the desired speed. Obviously this simplifies matters, because it avoids the necessity of providing for a variable alternating current frequency for starting purposes. FIGURE 6 shows the electrical drive and control circuits which produce the alternating current. Essentially it consists of a method of amplifying the power output from a fixed frequency oscillator and passing it through the proper network to give the two-phase alternating current for the motor field. The speed control, which at first sight may seem a bit complicated, is very reliable. A coil located at P in FIGURE 5 picks up two frequencies—one equal to the frequency of the A.C. drive in the motor and the other to the rotor speed. The "slip speed control" in FIGURE 6 amplifies the difference in these frequencies (called the slip frequency) and filters out all the others. This difference or "slip frequency" is rectified and applied to a volume control circuit in the drive in such a way that the slip frequency remains very constant. Since the oscillator frequency is constant to about five parts per million the rotor speed must remain as constant as the slip frequency. In practice we have found that with this control the rotor speed remained so constant that a special method of measuring it had to be devised. It was found that an ordinary household electrical clock with the field coils rewound could be made to run on the drive frequency. By comparing this clock with another operated by the "slip frequency" the rotor speed could be found with high precision. FIGURE 7 depicts a

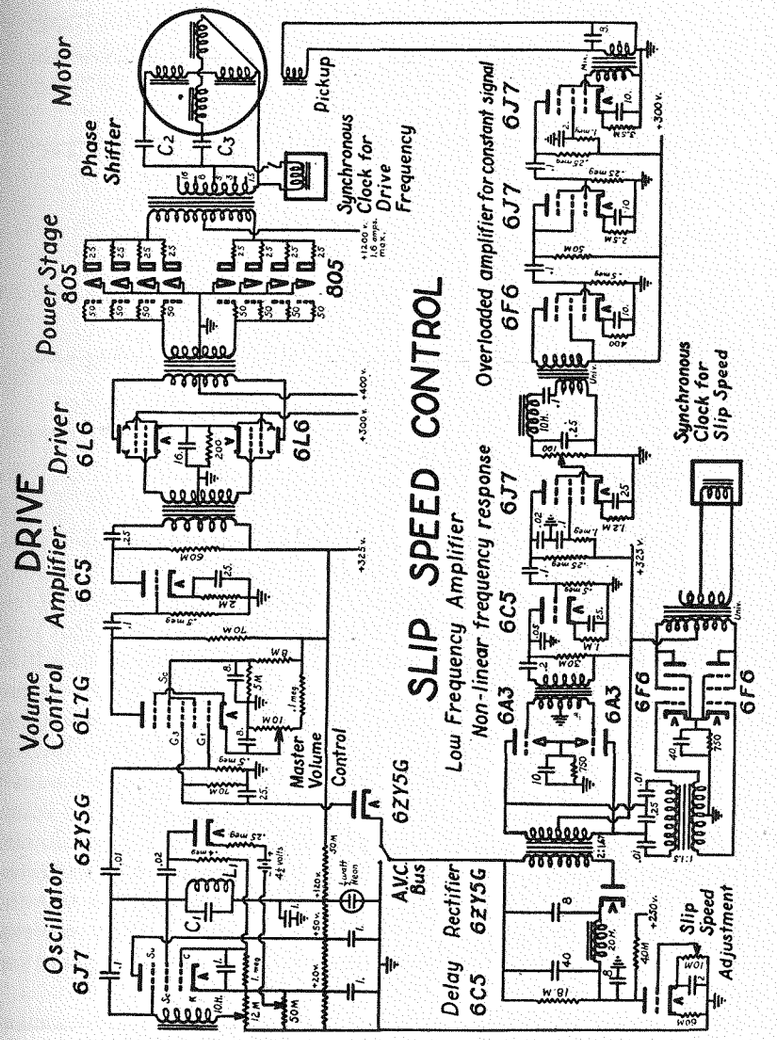

FIGURE 6. Centrifuge drive and control circuits. Resistance in ohms, M = 10^3 ohms and meg = 10^6 ohms; inductance in henries; capacitance in microforads. Drive frequency = 1188 cycles per second.

graph of the rotor speed for a period of ten hours, which shows that it is constant to 0.05 per cent over this time. When once set for a given rotor speed, it is only necessary for the operator to turn on the electrical power and start the vacuum pumps, etc., and the centrifuge will accele-

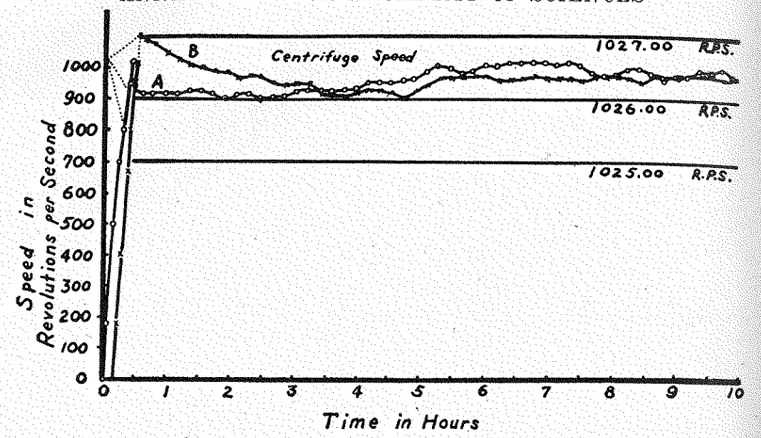

FIGURE 7. Two successive runs with slip speed control in operation. Drive frequency = 1188.0 cycles per second.

rate to the desired speed and remain constant to 0.05 per cent as long as desired without attention of the operator. When one wishes to stop the machine, the motor may be made to decelerate the machine to rest at the desired rate. In FIGURE 7 the curves, *A* and *B*, represent runs made on successive days without adjusting the apparatus. It will be seen that not only does the speed remain constant to one part in two thousand, but the machine will have the same speed within one part in two thousand in successive runs. Another advantage of this type of centrifuge is that, in case of failure of the control, the rotor speed cannot quite reach the drive frequency and thus can never explode the rotor.

With the 6-inch rotor in FIGURE 5, weighing about 9 lbs., one kilowatt input to the motor at a frequency of 1180 cycles per second accelerated the rotor to 1000 r.p.s. in 18 minutes, which compares favorably with the air drive. Our experience has shown that the electrical drive is superior to the air drive for the vacuum-type ultracentrifuge when freedom from attention and constant speed are required.

Before closing, it might be of interest to mention a new development in our laboratory at Virginia by which very great centrifugal forces are obtained. This development has been carried out principally by Holmes[16], Smith[17], and MacHattie[18]. The centrifuge is attached to a vertical iron rod which is suspended by the co-axial field of a solenoid. The current through the solenoid is regulated by the height of the rotor

[16] **Holmes, F. T.** Rev. Sci. Instr. **8**: 444. 1937.
[17] **Smith, C. S.** Rev. Sci. Instr. **12**: 15. 1941.
[18] **MacHattie, L. E.** Rev. Sci. Instr. **12**: 429. 1941.

so that as the rotor rises the current is decreased and when it falls the current increases. Consequently, the rotor is maintained at a constant height free from mechanical contact with anything. If the rotor is placed inside a vacuum and spun by a rotating magnetic field, the frictional torque on it is very small since there is no air friction and the magnetic support is almost friction-free due to the symmetry of the supporting magnetic field. Consequently, very high rotational speeds can be obtained with small rotors. MacHattie has spun a $\frac{3}{32}$-inch steel ball at 6,600,000 r.p.m., giving a centrifugal force of about 58 million times gravity. When this same ball was allowed to "coast" freely without the driving field at 6,000,000 r.p.m., it lost only 1 per cent of its speed in an hour, which shows how friction-free the magnetic support is.

In briefly summarizing this subject, there are at the present time methods of spinning rotors to their bursting points under controllable conditions. They may vary from $\frac{3}{32}$-inch diameter to as large a size as desired. Also, the centrifugal fields may be produced without remixing of the material. Indeed, for most problems one has a choice of several methods. However, in closing with these remarks, I do not want to give the impression that all the research on high-speed centrifuges has already been done. Due to their growing use, it is a safe guess that great advances in this technique will be made within the next few years.

OPTICAL PROBLEMS OF THE ULTRACENTRIFUGE

By W. B. Bridgman and J. W. Williams

From the Laboratory of Physical Chemistry, University of Wisconsin, Madison

Many of the methods of following the redistribution of components during sedimentation in an ultracentrifuge are based upon changes in optical properties. It is the purpose of this report to contrast and compare some of the more common methods. In order to do this the attempt has been made to summarize the fundamental principles involved in the several experimental assemblies. Also in the consideration of specific examples, answers to certain questions that are frequently raised in regard to the application of these methods have been given. This treatment is not an original approach to the optics involved, but is simply an application of conclusions arrived at in more exhaustive treatments by earlier workers. In particular the contributions of Lamm[1] and Svensson[2] have been used as the basis for this presentation. There are two general methods which have been developed, based upon absorption and refraction of light, respectively.

When the light absorption method is used the camera is focused on the cell and exposures at definite time intervals throughout the course of the experiment are made with monochromatic light of such wave length that it is absorbed by the sedimenting substance but not by the other components of the solution. After the completion of the experiment a set of exposures is taken to give a relationship between the blackening on the photographic plate and the concentration of the sedimenting substance. When the plate is microphotometered the relationship between the galvanometer deflection and the distance from the center of rotation is observed. From these diagrams and the concentration scale, figures for the concentration of the sedimenting substance at any point in the cell at several times are obtained.

In the scale method the camera is focused on a uniform linear scale (or its image), placed near the solution cell but on the side of the ultracentrifuge away from the objective lens and camera. As before, the exposures are made after definite intervals of time. With suitable refractive index increment the lines of the scale will be displaced by a concentration gradient in the cell. The scale line displacement is propor-

[1] **Lamm, O.** Nova Acta Soc. Sci. Upsala IV, **10** (6). 1937.
[2] **Svensson, H.** Kolloid Zeit. **90**: 141. 1940.

tional to the concentration gradient in the cell at a place corresponding to the position of that line. When line displacement is plotted as a function of distance from the rotation center, a curve results which gives the variation of the concentration gradient in the cell. To compute the concentration corresponding to a particular point in the cell, the area under the curve between that point and the surface from which the sedimentation takes place must be determined.

When a system contains more than one sedimenting substance, each component gives rise to a variation in concentration and in concentration gradient which appears in the sedimentation diagram. Whether variation in concentration or in concentration gradient is obtained depends upon the method of observation used in the experiment.

The refractive index method has so many important advantages over the light absorption procedure that it has in a sense rendered the latter obsolete. In its simplest arrangement in which a ruled scale is used, the method is tedious, and various attempts have been made to simplify the evaluation of the results. The Toepler schlieren method was introduced by Tiselius, Pedersen, and Eriksson-Quensel[3] to be used with the classical scale method for rapid and simple determinations of sedimentation constants. A boundary between solution and solvent appears on the photographic plate as a black band across the cell image. Philpot has described another scheme which is a combination of this schlieren method and the principle of Thovert[4] to give a direct photographic image of the sedimentation diagram. Other and more recent methods for the direct photography of concentration gradients which largely eliminate base-line difficulties have been described by Andersson, Longsworth and MacInnes, Svensson and others.

As a detailed discussion of the light absorption method and the problems encountered in its use has been given by Svedberg and Pedersen in their well-known monograph, it will suffice here to give only very brief statements about the procedure for evaluating sedimentation data. The method is attractive because the degree of blackening of a photographic plate can be simply and directly related to concentration in the cell when Beer's law is known to apply to the system.

To measure light intensity throughout the cell with a high degree of accuracy requires that close attention be paid to many details of technique. First, a light source is needed, preferably monochromatic, and having constant intensity with respect to both time and the space covered by the cell. To record the results photographically, the linear

[3] **Tiselius, A., Pedersen, K. O., & Eriksson-Quensel, I. B.** Nature **139**: 546. 1937.
[4] **Thovert, J.** Ann. Phys. **2** (9): 369. 1914.

portion of the characteristic curve of the photographic plate should be used. The plate must be developed by a carefully standardized technique. It is customary to make a "concentration scale" on each plate, composed of exposures through solutions of known concentration. These exposures serve as reference points for converting the observed blackening of the plate into concentration, since they have had the same treatment in development as the experimental exposures on the same plate. The density of the photographic image must be accurately photometered. A complete discussion of this method and the problems to be encountered has been given by Svedberg and Pedersen[5].

In the use of refractive index methods for following concentration gradients, there are three main problems to consider: (1) the variation of refractive index of the solution with the concentration of the solute; (2) the relation between the refractive index gradient and the deviation angle, δ, of a light ray passing through the region of the gradient; and (3) the optical method of measuring this deviation.

It is generally assumed that the refractive index can be expressed as a linear function of the concentration. Several investigators have found empirically that the refractive indices of colloidal systems can be expressed by linear relationships very satisfactorily.[6] These conclusions are based upon data from a wide range of systems including both inorganic suspensions and natural organic colloids (proteins, *et al*). In most cases the systems were studied in the range of concentration up to 0.03–0.04 grams per cc. It has been pointed out that the best agreement is obtained when the concentration is expressed in volume units.

In case the system being observed is polydisperse, it is important to consider if the refractive index increment (or absorption coefficient in light absorption methods) is a function of particle size. In many cases of homologous particles, independence of particle size is indicated. When it is possible to assume independence of particle size, it greatly simplifies the interpretation of results. Bailey, Nichols, and Kraemer have reported a method of interpreting results when particle size does affect the refractive index increment or the absorption coefficient[7].

In considering the path of the light through the region of refractive index gradient, it is qualitatively apparent that the light ray follows a path concave toward the region of higher refractive index. This is the

[5] **Svedberg, T., & Pedersen, K. O.** "The Ultracentrifuge." Clarendon Press. Oxford. 1940. pp. 240–253.
[6a] **Ostwald, W.** "Licht und Farbe in Kolloiden." Steinkopff. Dresden & Leipzig. 1924. pp 483–539.
[b] **Dumanski, A., & Putschkowski, B. S.** Kolloid Zeit. **48**: 338. 1929.
[7a] **Bailey, E. D., Nichols, J. B., & Kraemer, E. O.** Jour. Phys. Chem. **40**: 1149. 1936.
[b] **Svedberg, T., & Pedersen, K. O.** "The Ultracentrifuge." Clarendon Press. Oxford. 1940 pp. 338–342.

basic phenomenon for all refractive index methods of following concentration changes. The problem of determining the path of a light beam in a medium where the refractive index varies continuously in three dimensions is very difficult of general solution[8]. For certain special cases approximate solutions have been worked out. One such case is that in which the refractive index, n, is a function of only one coordinate, x. This case is of wide interest as it is the ideal situation resulting when diffusion, electrophoresis, or sedimentation occurs from an initially plane boundary. In 1893, Wiener[9] made an application of this method to diffusion gradients. More recently Lamm[1] has given the theory a fuller treatment. Not only is Lamm's treatment the basis of his scale method but it has also been used in the development of the various "schlieren" methods. Lamm gives as the expression for δ, the deviation angle observed outside the cell walls for a light ray passing through a cell of width, a, and having plane parallel walls:

$$\delta = a \frac{dn}{dx}. \qquad (1)$$

dn/dx is the refractive index gradient. In deriving this expression the assumptions have been made that all of the angles involved are so small that the angle itself may be used instead of its sine or tangent, and that both n and dn/dx can be considered as constant in the portion of the cell traversed by the ray.

The use of the angle in place of the sine will produce an error of about one part in 10,000 for an angle of 0.03 radian (*ca.* 1.7°) In the case of the tangent the error is about three parts in 10,000 for this same angle. Lamm has indicated this angle to be the limit within which experimental applications should be made. Certainly the error from this source is unimportant if the sum of all the angles involved is less than 0.03 radian. How well this condition is satisfied depends upon the particular experimental set up used; it will be considered in more detail in connection with the discussion of the optical systems.

The second assumption of constancy of n and dn/dx will be more closely approached the more nearly the light path through the cell approaches a straight line and the more nearly the angles of incidence and exit at the cell walls approach zero. This leads to the same conclusion as that of the previous paragraph, that the smaller all of the angles and curvatures involved in passing through the cell are kept, the greater is the applicability of the theory. Some calculations to be given

[8] **Gehrcke, E.** "Handbuch der physikalischen Optik." Barth. Leipzig. 1927. Vol. 1, Part 1, pp. 219–236.
[9] **Wiener, O.** Ann. Physik und Chemie. **49**: 105. 1893.

later, and based upon experimental observations with the scale method, lead to the conclusion that the assumption of constancy of n is justified in all cases, but at times the variation of dn/dx may be appreciable.

In the application of refractive index methods to sedimentation measurements in a centrifugal field, the further assumption is made that the optical treatment based upon plane surfaces of equal refractive index can also be applied to a case in which the surfaces of equal refractive index are actually concentric cylinder sections. In the Svedberg type of equipment in which measurements are made at a distance of 5 cm. or more from the center of rotation in which a sector opening of 2-3° is used, the approximation to plane surfaces is very good. The use of the above theory in connection with smaller rotors might be seriously questioned.

The scale displacement method of Lamm is undoubtedly the simplest optical method of recording the deviations of the light beams in passing through the cell. The principle of this method is illustrated in FIGURE 1. This is not a scale drawing but serves to illustrate the principles involved. The cell walls have been omitted for simplicity. A uniform scale is focused by the lens upon a photographic plate. The distances indicated by i, l, and b are optical distances, *i.e.*, the summation of the intervening geometric distances, each distance being divided by the refractive index of the respective medium traversed. The image of the scale on the plate is magnified by a factor G $(= i/l)$ and the center plane of the cell by the magnification factor H $(= G\,l\,/(l\text{-}b))$; H is the reciprocal of the projection factor F defined by Lamm.

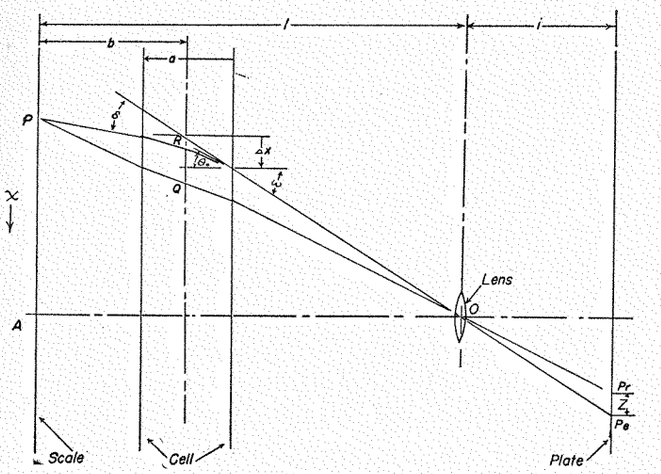

FIGURE 1

A reference exposure is made with the cell filled with the solvent medium. With this homogeneous material in the cell, a given scale line, represented by the point, P, in FIGURE 1, would be focused at Pr on the photographic plate. The central ray of light would follow some such path as $PQOPr$. When the experimental exposure is made with a concentration gradient in the cell (highest refractive index at the bottom of the cell) light from P would follow some such path as $PROPe$ being focused at Pe. (The focusing effect of the gradient is neglected here. Actually Pe will not be in the same plane as Pr. In practice this effect is minimized by using a lens of long focal length and small aperture.) The difference in position of Pr and Pe as determined by measurement in a comparator is called the scale displacement, designated by Z. The magnitude of Z is given by

$$Z = Gb\delta. \tag{2}$$

In order to relate this to the actual concentration we make use of the expression $dn/dx = dn/dc \cdot dc/dx$. For a linear variation of refractive index with concentration, dn/dc is a constant α for a given system. Combining this with equations (1) and (2) gives the over-all expression,

$$Z = G{\cdot}b{\cdot}a{\cdot}\alpha{\cdot}dc/dx, \tag{3}$$

which is used to relate Z to dc/dx. For many practical calculations, Z can be used directly without being converted into dc/dx. By suitable integration the actual concentration function can be determined.

As an illustration of the magnitudes of the quantities involved, the following data are given for an application of this method to an equilibrium centrifuge in the laboratory at the University of Wisconsin. Many of the conclusions to be drawn from these figures are not limited to this one method but may be useful in connection with other refractive index methods. The camera is arranged to give a scale magnification, G, of about two. The distances l and i (FIGURE 1) are about 2 and 4 meters respectively. The cell thickness, a, can be varied from 0.2 to 1.2 cm. The optical distance, b, from the center of the cell to the scale can be varied from 7 cm. to 20 cm. Experience has shown that the largest magnitude of Z that can be observed without undue blurring of the image is about 0.1 cm. (1000μ). By use of equation (2), the corresponding angle, δ, can be calculated. It is found to vary from 0.0064 radian (*ca* 20′) to 0.0033 radian (*ca* 10′) depending upon the value of b used. The other important angle is the angle of incidence, ω, upon the cell window. As the over-all height of the cell is about 2 cm. and the distance, l/b, is 210 cm., the maximum value of ω should be less than 0.01 radian. Both ω and δ are small enough to justify using the angle in place of its sine or tangent. In order to keep ω small, it is important to have the optic axis of the observing system pass through the center of the cell and to have the cell walls perpendicular to this axis. In electrophoresis or diffusion, where cells of the order of 10cm. in height may be employed, if convergent light is used in the cell, the center of convergence must be about 2 meters from the cell in order to keep ω less than 0.03 radian at the ends of the cell.

Lamm[10] has given for Δx, the increment of the x coordinate of the light path in passing through the gradient (FIGURE 1), the expression,

$$\Delta x = a\,\Theta_0 + \frac{a^2}{2n} \cdot \frac{dn}{dx}. \tag{4}$$

This can be put in the form

$$\Delta x = a\,\Theta_0 + a\,\frac{\delta}{2n}, \tag{5}$$

by combining it with equation (1). The change in refractive index, Δn, in the same region can be obtained by use of equations (5) and (1) as follows:

$$\Delta n = \frac{dn}{dx} \cdot \Delta x = \delta\,\Theta_0 + \frac{\delta^2}{2n} \cdot \tag{6}$$

In order to evaluate the change of dn/dx we need to have a value of d^2n/dx^2. By combining equations (1) and (2) and differentiating we obtain,

$$\frac{d^2n}{dx^2} = \frac{dZ/dx}{Gba}, \tag{7}$$

from which d^2n/dx^2 could be obtained with the aid of a Z vs x graph. Using equations (7) and (5) we obtain an expression for the variation of dn/dx over the light path.

$$\Delta\,\frac{dn}{dx} = \frac{d^2n}{dx^2} \cdot \Delta x = \frac{dZ/dx}{Gb}\,\Theta_0 + \frac{dZ/dx}{Gb}\,\frac{\delta}{2n}. \tag{8}$$

It is noteworthy that the expressions for Δn and $\Delta dn/dx$ are independent of the cell thickness, a. A given observed value of Z or dZ/dx will for a given optical arrangement correspond to a definite increment of n or dn/dx regardless of the cell thickness. Of course, in order to have the same values of Z and dZ/dx with cells of different thickness, the values of dn/dx and Δx could not be the same in both cells. In TABLE 1 are given results computed by the above equations for the values of $Z = 0.1$ cm., $Gb = 15.7$ cm., and $dZ/dx = 0.5$. This corresponds to a value of 0.0064 radian for δ. It must be recognized that the equations used are based upon the assumption of constancy of n and dn/dx and do not take into

[10] **Lamm, O.** Nova Acta Soc. Sci. Upsala IV, **10** (6): 13. 1937.

account the finite width of the light beam. Nevertheless, the results should be useful in indicating the magnitudes of the quantities involved. The numerical values were chosen to represent the maximum departures from ideal conditions encountered with this apparatus.

TABLE 1
LIGHT PATH DEVIATIONS

	$\Theta_0 = 0.01$ rad.		$\Theta_0 = 0$	
	$a = 1.2$ cm.	$a = 0.2$ cm.	$a = 1.2$ cm.	$a = 0.2$ cm.
$\frac{dn}{dx}$	0.0053	0.032	0.0053	0.032
Δx	0.0147	0.00243	0.0027	0.00043
Δn	0.000078	0.000078	0.000014	0.000014
$\Delta\frac{dn}{dx}$	0.00040	0.00040	0.00008	0.00008

This deals with aqueous solutions in which n is about 1.33. The value of Δn is so small that the assumption of constancy of n is certainly justified. The value of $\Delta\ dn/dx$ approaches 10 per cent of dn/dx in the case of the thicker cell. A comparison of the results for the different values of Θ_0 shows that the angle of incidence of the light upon the cell can make the major contribution to the variation of n and dn/dx in the light path. Of course, Θ_0 will always be less than ω if the cell is filled with a more highly refracting medium than the surrounding space. The table shows that although the bending of the light ray alone ($\Theta_0 = 0$) does not make $\Delta\ dn/dx$ large enough to affect seriously the assumption of constancy of dn/dx, an angle of entrance into the solution of only 0.01 radian makes $\Delta\ dn/dx$ a very appreciable part of dn/dx. In a large diffusion or electrophoresis cell the concentration gradient is frequently confined to the central portion of the cell where Θ_0 will be small if the cell is properly placed in the optical set up. The larger values of Θ_0 at the edges will be associated with regions where dn/dx is small and thus do not contribute a serious error to the measurements. The figures in TABLE 1 illustrate the desirability of using a thin cell where high gradients are concerned.

In boundary experiments such as sedimentation velocity, diffusion and electrophoresis, maximum values of Z and dZ/dx will not occur at the same point in the cell as implied in the above calculation. Maximum values of these quantities do occur together in sedimentation equilibrium experiments.

The apparatus described is unusual in that a large distance, b, is used. The sedimentation velocity equipment at the University of Wisconsin is more typical of applications for observing boundaries between solution

and solvent. Here the distance b can be varied from 0.75 cm. to 11.75 cm. and the corresponding factors for Gb vary from 1.3 to 19.2. If b is 0.75 cm. and Z is 0.1 cm., δ equals 0.0775 radian. In practice this small value of b is rarely used. In sedimentation velocity experiments we have found it quite unusual for Z to be as great as 0.05 cm. Under actual working conditions the maximum values of δ are of the same order of magnitude as in the sedimentation equilibrium apparatus. In electrophoresis cells the thickness, a, is frequently much greater than in the above example.

The Lamm scale method does have the disadvantage of requiring considerable laborious routine work in measuring the position of each scale line and in plotting the values of Z. These disadvantages have led to devising optical arrangements which give directly the curve of dn/dx vs x on the photographic plate. In FIGURE 2 is a schematic diagram of a typical schlieren apparatus adapted from Svensson.[2] The direction of the gradient is assumed to be vertical The light source may be either a horizontal slit producing a bright line image, or it may be a straight edge resulting in the final curve being given as a boundary between light and dark. The schlieren lens must be large enough in diameter to light the cell uniformly. It forms a real image of the source upon the inclined slit. The objective lens focuses the cell upon the photographic plate. The cylindrical lens with vertical axis has no focusing effect on light in the vertical plane so that each vertical coordinate on the photographic plate corresponds to a definite position, x, in the cell. This is expressed by

$$X = Gx, \tag{9}$$

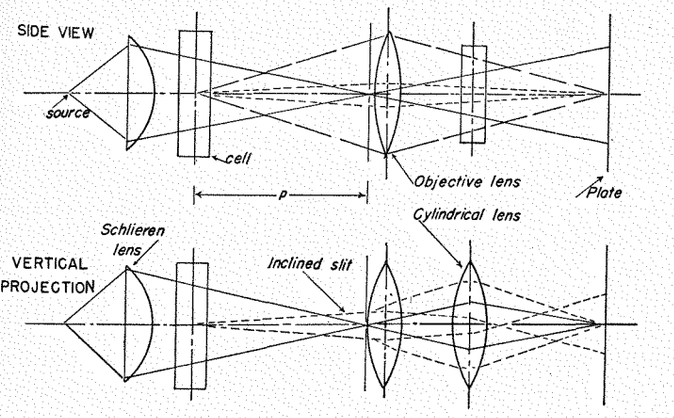

FIGURE 2

where G is the magnification of the cell on the plate, x is the vertical coordinate in the cell and X the vertical coordinate on the plate. In a horizontal plane the combined effects of the objective lens and the cylindrical lens focus the inclined slit upon the plate with a magnification, E. In this plane the cell is out of focus. Since all the light in the system comes from the source and through the slit, as indicated by the heavy lines in FIGURE 2, there is a straight vertical line formed on the plate in the absence of any gradient.

The presence of a gradient will cause the image of the light source on the inclined slit to be displaced as indicated in FIGURE 3. The point of

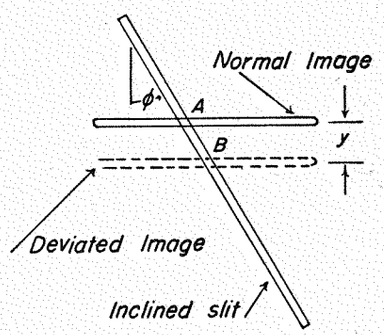

FIGURE 3

intersection of the slit and the image is changed from A to B. The transverse component of this difference is focused on the plate by the cylindrical lens. This causes the image to be horizontally displaced a distance Y, which is given by the expression

$$Y = E \cdot y \cdot \tan \phi. \tag{10}$$

In turn, y, the vertical displacement of the image at the inclined slit, is given by

$$y = k \cdot \delta, \tag{11}$$

where k is a proportionality factor depending upon the optical arrangement and δ is the same as defined in equation (1).

Other applications of the schlieren method may involve the use of additional lenses or change the order in which the various parts are placed, but the essential principles involved are illustrated by the above example. Svensson[2] has given a thorough treatment of the optical theory of these methods and the factors affecting their sensitivity and accuracy.

In TABLE 2 are given some values of y and δ calculated for different observed displacements and various angles of the inclined slit. The assumptions are made that $E = 1.0$ and $k = 100.0$ cm. It is to be noted that for the larger values of ϕ under the conditions chosen, the values of δ are of the same order of magnitude mentioned in connection with the scale method. The use of other E values would inversely influence the values given. The physical significance of k will vary with the optical system used. For the arrangement illustrated in FIGURE 2, k is the optical distance, p. The values in TABLE 2 correspond to p equal to one meter. If a lens is used between the cell and the inclined slit, k will in general be some function involving the focal length of the lens[2]. Whatever its significance it would appear that k should be large so that δ is small.

TABLE 2

DISPLACEMENTS FOR SCHLIEREN METHOD

E = 1m.; k = 100; y in cm.; δ in radians.

	$\phi = 20°$		$\phi = 45°$		$\phi = 60°$	
Y_{cm}	y	δ	y	δ	y	δ
2	5.50	0.0550	2.00	0.0200	1.154	0.01154
1	2.75	0.0275	1.00	0.0100	0.577	0.00577
0.5	1.38	0.0138	0.50	0.0050	0.289	0.00289

In all of the methods, *i.e.*, absorption, scale, and schlieren, it is necessary to relate the observed value of the concentration or of dn/dx to the corresponding position in the cell. This problem has been considered by Wiener[9], Lamm[1], and Svensson[2]. The situation is summarized in FIGURE 4. The actual light path of the deviated ray is indicated by $ABCD$. This curve will be represented by the equation

$$x = z\Theta_0 + \frac{z^2}{2n}\frac{dn}{dx} \tag{12}$$

to the extent that the assumptions of the constancy of n and dn/dx are valid. The observed deviation of the ray will correspond to a value of dn/dx given by equation (1). Svensson has shown that this value of dn/dx will occur at a value of x corresponding to a point on the curve between the limits B and C. The light entering the camera appears to have come along the path, $AEFG$. In the use of the scale method, the values of Z are plotted against the position of the line on the deviated (or experimental) scale. The position in the cell is then computed from this graph by use of the magnification factor of the cell upon the photographic plate. In the schlieren method the camera is focused on the center of the cell and the magnification factor is used to determine the position in the

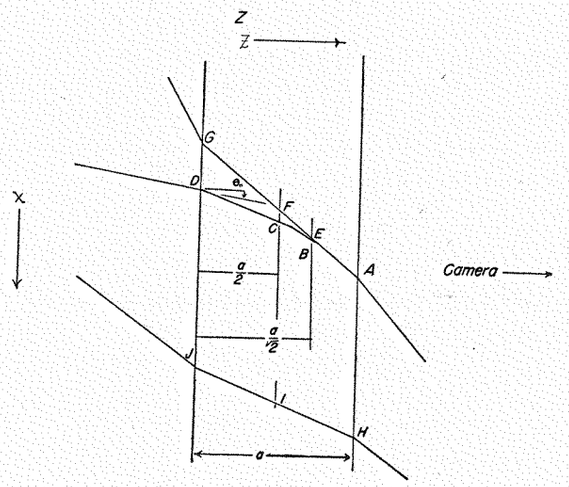

FIGURE 4

cell. Both of these methods will result in the value of dn/dx belonging to any value of x between B and C being assigned to the value of x associated with the point, F. The distance, FC, was first shown by Wiener to be $\frac{a}{8n}\frac{dn}{dx}$. Substituting the data of TABLE 1 in this expression gives a value for FC of 0.00074 cm. for the 1.2 cm. cell, and of 0.00013 cm. for the 0.2 cm. cell. These values are so small that it is unnecessary to correct for them. The use of a magnification factor corresponding to a position in the cell a little closer to the camera would reduce this error further. Thus Svensson suggests $a/\sqrt{3}$ as an optimum value. He also arrives at the conclusion that the error due to the use of convergent light is at a minimum for a value of z near $a/2$.

The same error would appear to be inherent in the light absorption method. A concentration gradient is almost invariably accompanied by a refractive index gradient. As a result the light that appears to have passed through the cell by the path, AG, will actually have followed the path, AD.

In the scale method the light path for the same scale line would in the reference scale traverse the cell in the path, HIJ. If the values of Z were plotted against the line position in the reference scale (or against the line number,) the value of dn/dx would be assigned to a value of x corresponding to the point, I. The incorrectness of this procedure was pointed out by Lamm.

It is to be understood from the remarks up to this point that the determination of the sedimentation velocity is independent of the exact position of the real base line or line of zero scale displacement. This will not be true when it is desired to compute the concentration of a homogeneous substance which is sedimenting. This concentration in case the scale method is used is given by the expression

$$C_0 = \frac{FA_1}{B_z B_x G a b \alpha}\left(\frac{X_1}{X_0}\right)^2, \qquad (13)$$

in which

F is the projection factor with which the cell is photographed when the camera is actually focused on the scale (or scale image).

A_1 is area measure in cm² between the line displacement-distance curve and the base line (line of zero displacement). It varies with the scale distance.

B_z and B_x are magnification factors for ordinate and abscissa.

G is the enlargement factor with which the scale image is photographed.

a is the cell thickness.

b is the optical distance between scale and the middle of the cell.

α is the refractive index increment.

X_0 and X_1 are the distances from the axis of rotation to the meniscus and to the bisector of the maximum in the displacement-distance curve, respectively.

Obviously the same value for C_0 should be found as the distance of the boundary from the center of rotation increases. Decreasing values of C_0 with increasing boundary distance indicate the occurrence of convection which might be caused by temperature variation or by deformation of the sectorial part of the cell during the experiment. In these ways the dilution factor (X_1/X_0) is rendered invalid.

The determination of the enlargement factors, F and G, and the cell thickness, a, does not involve any particular difficulty. The constant, G, is evaluated by comparing the line interval on the scale pictures obtained at low speed with the known line distance on the scale itself. Under ordinary circumstances the optical distance, b, is determined photographically, and since the accuracy by using this procedure is about 1 mm., the estimate of the concentration from the area under the displacement curve will not be very accurate at short scale distances.

This constant, b, may be calculated to a precision of about 0.1 mm. by studying the variation of the area under the curve with scale distance. The cell is filled with a solution of high molecular weight substance of

such concentration that good scale photographs are obtained with $b = 1.0 - 2.0$ cm. and with the boundary halfway down in the cell. When a number of scale pictures with different scale distances are taken at the same time, the ratio FA/Gb is constant and independent of b. If, therefore, values of FA/G for the different distances of b are plotted as a function of the measured displacement of the projection system, the position for $b = 0$ is found from the graph.

A knowledge of the exact position of the base line is indispensable for all measurements which involve an integration and for the calculation of molecular weights from the sedimentation equilibrium. This is also generally but not necessarily true of diffusion measurements. Lack of such knowledge is probably in large measure responsible for those discrepancies between analytically determined and calculated solute concentrations which have been reported in the literature[11].

Other reasons for difficulties of this sort have been mentioned. Thus, it has been suggested that sedimenting asymmetrical molecules may be oriented and thus show an abnormal refractivity. This suggestion is of interest because it is sometimes stated that the calculation of molecular weights by the usual combination of sedimentation velocity and diffusion data is attended by some uncertainty for the same reason.[12] It is contended, "one might expect some molecules to behave differently in the diffusion process and in the sedimentation process so that the same fractional coefficient cannot be used to describe both phenomena . . . Sedimentation is due to the superposition of an external field on Brownian motion and can produce a preferred orientation . . . giving rise to a different coefficient."

In order to discover whether an orientation of asymmetrical molecules to give abnormal refractivities and abnormal sedimentation rates will result during the performance of the experiment, one must answer the question, how does the energy which such molecules acquire because of the centrifugal field compare in magnitude with kT? It can be shown that during the sedimentation in centrifugal fields available in the modern ultracentrifuge of proteins such as those for which Svedberg and Pedersen give molecular constants in their tables, the kinetic energy of the sedimenting units, $mv^2/2$, is very small compared to kT. In other words, the effect of any orientation in these cases may be neglected and it could not account for differences between analytical and calculated solute concentrations.

The variation of area under the line displacement-distance curve with

[11] **McFarlane, A. S.** Biochem. Jour. **29**: 407. 1935.
[12] **Beckmann, C. O., & Landis, Q.** Jour. Am. Chem. Soc. **61**: 1495. 1939.

change in scale distance can be computed so that it need not be considered here as a source of error in concentration determinations.

It should be noted that the use of equation (13) is not restricted to the case in which a single homogeneous substance is present. In a mixture of several components with sufficiently different sedimentation constants, the concentration of each single component may be calculated from the area under the corresponding peak of the diagram, provided the refractive index increment is known for each sedimenting substance. If the individual curves are not completely resolved, it is sometimes possible to analyze the resultant diagram to give the individual curves. If one side of the composite curve is normal in shape, the complete individual curve may be constructed about the most probable bisector line drawn at right angles to the base line for the particular peak. The constructed curve is now subtracted from the experimental diagram. The remaining curve is treated in a similar way until the whole experimental curve is divided up into individual curves. The middle or bisector line for the several curves should always form a right angle with the base line. Such a construction for individual curves can be carried out only when the resolving power of the ultracentrifuge is sufficiently great, so that the bisector line for one curve is not crossed by any of the other individual curves. As an illustration of the application of these methods to determinations of concentrations as well as of sedimentation rates in a system of several components, reference is made to a recent article of Petermann[13], which describes work having to do with the pepsin digestion of serum globulins.

Theoretically, scale and schlieren methods can be made to fit the conditions of the analysis equally well. For a comparison of results obtained by the two refractometric methods, reference may be made to diffusion studies with egg albumin and to sedimentation and diffusion studies with ribonuclease. Longsworth[14] has made a study of the influence of pH on the diffusion of egg albumin by using the schlieren scanning method in photographing the refractive index gradients as the blurring of the boundaries progresses. Within the usual pH stability region, average values of the diffusion constant corrected to a process taking place in pure water at 0°C. vary between 3.96 and 4.13 x 10^{-7}. Measurements of Polson[15] made by using the Lamm scale method give $D = 4.00 \times 10^{-7}$ when the result has been computed for 0°C. The agreement is excellent. In a sense, however, this is not a completely rigorous test case because protein solutions of 1.4 per cent were used in

[13] **Petermann, M. L.** Jour. Phys. Chem. **46**: 183. 1942.
[14] **Longsworth, L. G.** Ann. N. Y. Acad. Sci. **61**: 267. 1941.
[15] **Polson, A.** Kolloid Zeit. **87**: 149. 1939.

the experiments and because egg albumin molecules are either spherical or nearly spherical in shape.

In another recent series of observations Rothen[16] has used the position and areas of schlieren diagrams to evaluate the sedimentation and diffusion constants for purified crystalline ribonuclease. The result found from these measurements for the molecular weight of the protein is 13,000. From sedimentation velocity and diffusion experiments performed here by using the Lamm scale method an appreciably higher molecular weight for the experiments has been found. It will be noted that partial specific volume data also are not entirely in agreement, contributing to the differences. A summary of the results from the two sources, computed to a comparable basis, are presented in TABLE 3.

TABLE 3
CHARACTERISTIC CONSTANTS FOR RIBONUCLEASE

	Rothen	*University of Wisconsin*[17]
V	0.71	0.73 – .74
s_{20}	2.09 x 10^{-13}	2.15 x 10^{-13}
D_{20}	12.5 x 10^{-7}	10.2 x 10^{-7}
M	13,000	~ 17,000

It should be pointed out that samples of ribonuclease from different stocks were used in the two laboratories. The crystalline preparation used here was supplied through the kindness of Dr. M. Kunitz, of The Rockefeller Institute for Medical Research, Princeton, New Jersey. It had stood in the dry condition for some weeks and it is quite possible it had undergone some denaturation on standing. If such denaturation leads only to configurational change, some modification in the values of s and D is to be expected, but the ratio of the two constants should not vary and the molecular weight result would be unchanged.

Apart from consideration of the optical problems of the ultracentrifuge, the following suggestion is made. Some of the important modern methods of studying high molecular weight substances have been the result of researches of Svedberg. The ultracentrifuge, developed by him, is the most powerful tool for the study of the mass behavior of such substances. It is proposed to honor him on this occasion by designating as the Svedberg the unit of the specific sedimentation constant, *i.e.*, the rate in centimeters per second at which the boundary moves under unit centrifugal field, multiplied by 10^{13}. It is further proposed that the capital letter S be used as its symbol.

[16] **Rothen, A.** Jour. Gen. Physiol. **24**: 203. 1940.
[17] **Vilbrandt, C. F., Tennent, H. G., & Hakala, N. V.** Unpublished.

THE INTEGRATION OF THE DIFFERENTIAL EQUATION OF THE ULTRACENTRIFUGE

BY W. J. ARCHIBALD

From the Division of Physics and Electrical Engineering, National Research Council, Ottawa, Canada.

I

If a dilute solution be placed in a gravitational field of force, the distribution of concentration changes from an initial uniform distribution to an exponential one. Theoretically, it will require an infinite time for this final equilibrium distribution to be established; actually, it will be achieved to a high degree of approximation in a finite time. It is the object of this paper to show how to calculate the concentration as a function of position in a gravitational field of force for all values of the time, t, and hence to enable one to decide how far conditions differ from the equilibrium condition at any particular time.

For the case of a dilute solution in a centrifugal field of force the information desired is to be obtained by solving the following differential equation:

$$\frac{1}{r}\frac{\partial}{\partial r}\left\{\left(D\frac{\partial c}{\partial r} - \omega^2 rsc\right)r\right\} = \frac{\partial c}{\partial t}. \qquad (1)$$

In this equation, r is the distance from the center of rotation to any point of the solution, c the concentration at that point, ω the angular velocity of rotation, D the coefficient of diffusion, and s the sedimentation velocity of the dissolved substance. This equation was first derived by Lamm[1] as follows: consider an elementary volume of the solution of unit depth and bounded by two cylindrical surfaces at a distance r and $r + dr$ from the axis of rotation. If c is the concentration at the surface, r, then the net quantity of dissolved substance crossing this surface in an outward direction in unit time is

$$Q = \left(\omega^2 rsc - D\frac{\partial c}{\partial r}\right)2\pi r, \qquad (2)$$

and the net accumulation of substance per second in the layer of thickness, dr, is $-(\partial Q/\partial r)\,dr$, which is also represented by $\partial c/\partial t\, 2\pi r\, dr$. The differential equation (1) is obtained by equating these two quantities.

Lamm, O. Ark. Mat. Astron. Fysik. **21B**: No. 2. 1929.

Several mathematical discussions of this equation are to be found in the literature.[2]

Before proceeding to the mathematical discussion of equation (1) it must be stated that in what follows it will be assumed that D and s are constants (*i.e.*, they are independent of c), and this implies that we are dealing with an ideal, dilute solution in which no combination occurs between components of the solution and in which the effects of electric charge, if any, are properly repressed.

For molecular weight determinations in an ultracentrifuge the substance to be studied is placed in a cell with radial sides and two bounding cylindrical ends. The solutions of equation (1) in which we are interested are those which refer to a cell of this type.

In order to make the discussion of equation (1) as straightforward as possible, let us first carry through the treatment in a formal manner and not be concerned with the specific details of the functions and symbols which may appear.

II

The formal treatment proceeds as follows: in equation (1) let

$$c(r,t) = RT,$$

where R is a function of r alone, and T is a function of t alone. On substitution this gives

$$\frac{1}{rR}\frac{d}{dr}\left\{\left(D\frac{dR}{dr} - \omega^2 rsR\right)r\right\} = \frac{1}{T}\frac{dT}{dt}.$$

In this equation the variables are separated and consequently each side can be equated to a constant, β, giving the two equations

$$\frac{1}{T}\frac{dT}{dt} = -\beta, \tag{3}$$

and

$$\frac{1}{rR}\frac{d}{dr}\left\{\left(D\frac{dR}{dr} - \omega^2 rsR\right)r\right\} = -\beta. \tag{4}$$

From equation (3)

$$T = e^{-\beta t}.$$

Equation (4) may be written in the form

$$\frac{d^2R}{dr^2} + \left(\frac{1}{r} - \delta r\right)\frac{dR}{dr} + \sigma R = 0, \tag{5}$$

where

$$\delta = \frac{\omega^2 s}{D} \quad \text{and} \quad \sigma = \frac{\beta - 2\omega^2 s}{D}.$$

[2] [a] **Faxen, H.** Ark. Mat. Astron. Fysik. 21B: No. 2. 1929; [b] **Oka, S.** Proc. Physico-Math. Soc. Japan. **19**: 1094. 1937.

Thus we have

$$c(r,t) = R(r)e^{-\beta t}, \tag{6}$$

where $R(r)$ is a solution of equation (5) and β is an undetermined constant. Equation (5) can be transformed into an equation containing only one parameter by changing the independent variable from r to z where

$$z = \frac{\partial r^2}{2}.$$

Then equation (5) becomes

$$\frac{d^2M}{dz^2} + \left(\frac{1}{z} - 1\right)\frac{dM}{dz} - \frac{\alpha}{z}M = 0, \tag{7}$$

where M is the function of z which corresponds to R as a function of r and where

$$\beta = 2\omega^2 s\,(1 - \alpha).$$

Thus equation (6) may be written in the form

$$c(z,t) = M(z)e^{(\alpha-1)\tau} \tag{8}$$

where

$$\tau = 2\omega^2 st.$$

In equation (8) $M(z)$ is any solution of equation (7) and α is an undetermined constant. For the most general case we have from the theory of differential equations

$$M(z) = AF(z) + BW(z), \tag{9}$$

where A and B are constants and $F(z)$ and $W(z)$ are two independent solutions of equation (7). Thus equation (8) contains three constants, *viz.*, A,B and α, and these are to be determined by one initial condition and two boundary conditions. These conditions are

(a) at $t = 0$, $c(z,0) = c_0$, a constant, for all values of z;

(b) no dissolved substance can flow through either end of the cell containing the liquid.

Condition (b) can be formulated in mathematical language by recalling that the net flow through any cylindrical surface at a distance, r, from the center of rotation is given by equation (2). Thus Q must equal zero for $r = r_1$ and $r = r_2$, where r_1 and r_2 are the co-ordinates of the inner and outer bounding surfaces, respectively. Thus condition (b) requires that

$$D\frac{\partial c}{\partial r} - \omega^2 rsc = 0 \qquad \text{for } r = r_1 \text{ and } r_2,$$

or in terms of the variable, z

$$\frac{dM}{dz} - M = 0 \qquad \text{for } z = \left\{\begin{matrix}\frac{\partial r_1^2}{2} \\ \frac{\partial r_2^2}{2}\end{matrix}\right\} = \left\{\begin{matrix}a \\ b\end{matrix}\right\}. \tag{10}$$

Since $M(z)$ is given by equation (9), the condition (10) leads to the following requirements:

$$A\{F'(a) - F(a)\} + B\{W'(a) - W(a)\} = 0, \quad (11a)$$

$$A\{F'(b) - F(b)\} + B\{W'(b) - W(b)\} = 0, \quad (11b)$$

where the prime denotes differentiation with respect to z. Now the system of equations (11a) and (11b) can have roots other than the trivial ones $A = 0$, $B = 0$ only if

$$\begin{vmatrix} F'(a) - F(a), & W'(a) - W(a) \\ F'(b) - F(b), & W'(b) - W(b) \end{vmatrix} = 0. \quad (12)$$

Since both the F and W solutions of equation (7) will contain the parameter α, we have in equation (12) the relation from which the permissible values of α are obtained. Equation (12) has an infinite set of roots: any root of this equation will be designated by α_n, where n is any positive integer between 0 and ∞.

For any value of α_n there is a corresponding value of A_n and B_n which can be obtained from equations (11). We can determine one of these constants in terms of the other, *e.g.*, from equation (11a) we have

$$B_n = -\frac{F_{\alpha_n}'(a) - F_{\alpha_n}(a)}{W_{\alpha_n}'(a) - W_{\alpha_n}(a)} = -K_n A_n.$$

(It is now necessary to add the subscript α_n to the F and W functions).

As a result of the above discussion it is now obvious that $c(z,t)$ is given by

$$c(z,t) = \sum_{n=0}^{\infty} A_n M_{\alpha_n}(z)\, e^{(\alpha_n - 1)\tau}, \quad (13)$$

where $$M_{\alpha_n}(z) = F_{\alpha_n}(z) - K_n W_{\alpha_n}(z).$$

Only the quantities A_n ($n = 0, \ldots \infty$) are left undetermined, and to evaluate them we call upon the first boundary condition, *viz.*, for $t = 0$

$$c(z,0) = c_0 = \sum_{n=0}^{\infty} A_n M_{\alpha_n}(z).$$

Multiply both sides of this equation by $e^{-z} M_{\alpha_n}(z)$ and integrate from $Z = a$ to $Z = b$. This gives

$$c_0 \int_a^b e^{-z} M_{\alpha_n} dz = \sum_{m=0}^{\infty} A_n \int_a^b e^{-z} M_{\alpha_m} M_{\alpha_n} dz. \quad (14)$$

The integral on the right of equation (14) may be written

$$\int_a^b e^{-z} M_{\alpha_m} M_{\alpha_n} dz = \frac{1}{\alpha_m} \int_a^b e^{-z} M_{\alpha_m} \left\{ z \frac{d^2 M_{\alpha_m}}{dz^2} + (1 - z) \frac{dM_{\alpha_m}}{dz} \right\} dz, \quad (15)$$

since M_{α_m} is a solution of equation (7). Integration by parts of the right hand side of equation (15) gives, after considerable manipulation,

$$\int_a^b e^{-z} M_{\alpha_m} M_{\alpha_n} dz = \frac{1}{\alpha_m - \alpha_n} \left[z e^{-z} \left\{ M_{\alpha_n} \left(\frac{dM_{\alpha_m}}{dz} - M_{\alpha_m} \right) - M_{\alpha_m} \left(\frac{dM_{\alpha_n}}{dz} - M_{\alpha_n} \right) \right\} \right]_a^b. \quad (16)$$

But at the points, a and b

$$\frac{dM_{\alpha_n}}{dz} - M_{\alpha_n} = \frac{dM_{\alpha_m}}{dz} - M_{\alpha_m} = 0,$$

since α_m and α_n are values of α which satisfy equation (10). Thus for the allowed values of α we have

$$\int_a^b e^{-z} M_{\alpha_m} M_{\alpha_n} dz = 0 \qquad m \neq n.$$

If $m = n$, the above expression gives for the integral an indeterminate form, which will be evaluated later.

From equation (14) it is now evident that the coefficient A_n is

$$A_n = \frac{c_0 \int_a^b e^{-z} M_{\alpha_n} dz}{\int_a^b e^{-z} \{M_{\alpha_n}\}^2 dz}.$$

Thus the final expression for $c(z,t)$ with all the constants determined, is

$$c(z,t) = c_0 \sum_{n=0}^{\infty} \left[\frac{\int_a^b e^{-z} M_{\alpha_n}(z) dz}{\int_a^b e^{-z} \{M_{\alpha_n}(z)\}^2 dz} M_{\alpha_n}(z)\, e^{(\alpha_n - 1)\tau} \right] \quad (17)$$

where the α_n's are the roots of equation (12).

III

The formal treatment of the equation is now complete. Before the results can be used for purposes of computation it is necessary to specify the functions $F(z)$ and $W(z)$, which are the two independent solutions

of equation (7). This involves a careful study of equation (7), which is most conveniently made by writing the equation in the more general form,

$$\frac{d^2M}{dz^2} + \left(\frac{\gamma}{z} - 1\right)\frac{dM}{dz} - \frac{\alpha}{z}M = 0, \tag{18}$$

where γ can take only integral values. As there are now two parameters it is necessary to write the functions $F(z)$ and $W(z)$ as $F(\alpha;\gamma;z)$ and $W(\alpha;\gamma;z)$ in the subsequent discussion.

The simplest solution (the one that is bounded at the origin) is the well known confluent hypergeometric series, *viz.*,

$$F(\alpha;\gamma;z) = 1 + \frac{\alpha}{1.\gamma}z + \frac{\alpha(\alpha+1)}{1.2\gamma(\gamma+1)}z^2 + \cdots\cdots \tag{19}$$

A list of recurrence formulae has been given for this function by Webb and Airey.[3]

Several methods are available for determining a second solution of $W(\alpha;\gamma;z)$, but not all of them lead to forms which are useful. Perhaps the best method is to express $F(\alpha;\gamma;z)$ as a contour integral and study the integral thus obtained. To do this we make use of the theorem that

$$\frac{1}{m!} = \frac{1}{2\pi i}\int_C e^t t^{m-1}\,dt, \tag{20}$$

where the contour, C, is any closed path in the t plane encircling the origin once in a counterclockwise direction. Now F may be expressed in the following form:

$$F(\alpha;\gamma;z) = (\gamma-1)!\sum_{n=0}^{\infty}\frac{c_n z^n}{(\gamma+n-1)!},$$

where c_n is the coefficient of x^n in the expansion of $(1-x)^{-\alpha}$. Therefore, by means of equation (20), we have, putting $m = b + n - 1$

$$F(\alpha;\gamma;z) = \frac{(\gamma-1)!}{2\pi i}\sum_{n=0}^{\infty}c_n z^n\int_C e^t t^{-\gamma-n}\,dt. \tag{21}$$

If we now choose the path, C, so that on all points of it $|z/t| < 1$, then we may reverse the order of summation and integration, the series being convergent for all values of t. Hence,

$$F(\alpha;\gamma;z) = \frac{(\gamma-1)!}{2\pi i}\int_{C'}\left(1-\frac{z}{t}\right)^{-\alpha}e^t t^{-\gamma}\,dt. \tag{22}$$

By virtue of equation (21), the path of integration, C', must encircle the point $t = z$. Therefore, C' can be deformed into any closed path which encircles the points $t = 0$ and $t = z$. It is further clear that the integrand is a single-valued function of t if a cut be made between the points, $t = 0$ and $t = z$.

Let us now deform C' into the path shown in FIGURE 1. Owing to the factor e^t in the integrand, those parts of C' for which t is large and negative contribute very little to the integral. If we make the part of C'—marked A in FIGURE 1—tend to an infinite distance from the imaginary

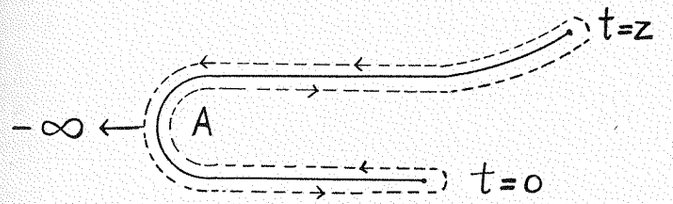

FIGURE 1

axis, then equation (22) may be replaced by the sum of two integrals, one around the upper loop and the other around the lower. Therefore,

$$F(\alpha;\gamma;z) = W_1(\alpha;\gamma;z) + W_2(\alpha;\gamma;z),$$

where

$$W_1(\alpha;\gamma;z) = \frac{(\gamma-1)!}{2\pi i}\int_{C_0}\left(1-\frac{z}{t}\right)^{-\alpha}e^t t^{-\gamma}\,dt$$

and C_0 comes from $-\infty$, encircles the origin in a counterclockwise direction and returns to $-\infty$; W_2 is given by the same integral and a path C_z which encircles the point, $t = z$.

It can be shown that W_1 and W_2 are two independent solutions of equation (18).[4]

It is a simple matter to obtain the asymptotic expansion of W_1 and W_2 for large values of z. We express W_1 as

$$W_1(\alpha;\gamma;z) = \frac{\Gamma(\gamma)}{2\pi i}(-z)^{-\alpha}\int_{C_0}\left(1-\frac{t}{z}\right)^{-\alpha}e^t t^{\alpha-\gamma}\,dt,$$

and now the integrand may be expanded by the binomial theorem for sufficiently large values of z. Carrying out this step and using equation (20) we find

$$W_1(\alpha;\gamma;z) \backsim \frac{\Gamma(\gamma)}{\Gamma(\gamma-\alpha)}(-z)^{-\alpha}\,G(\alpha;\alpha-\gamma+1;-z), \tag{23a}$$

[3] **Webb, H. A., & Airey, J. R.** Phil. Mag. & Jour. Sci. **36**: 129. 1918.

[4] **Whittaker, E. T., & Watson, G. N.** "A Course of Modern Analysis." 4th edit. Cambridge Univ. Press. 1927. p. 343.

where G denotes the semi-convergent series

$$G(\alpha;\gamma;z) = 1 + \frac{\alpha\gamma}{1!z} + \frac{\alpha(\alpha+1)\gamma(\gamma+1)}{2!\,z^2} + \cdots\cdots$$

To find the asymptotic expansion of W_2 we make the substitution $t - z = u$ and proceed as above. One gets

$$W_2(\alpha;\gamma;z) \backsim \frac{\Gamma(\gamma)}{\Gamma(\alpha)} e^z z^{\alpha-\gamma} G(1-\alpha;\gamma-\alpha;z). \tag{23b}$$

These expressions are useful for purposes of computation for large values of z.

It is now necessary to obtain from W_1 and W_2 a convenient second solution of equation (18). This is largely a matter of trial and error; the following method of approach is only one of many.

From $W_1(\alpha;\gamma;z)$ let us form a new function $W_s(\alpha;\gamma;z)$ as follows

$$W_s(\alpha;\gamma;z) = (-1)^{\alpha+\gamma} W_1(\alpha;\gamma;z). \tag{24}$$

The asymptotic expansion of W_s is, using equation (23)

$$W_s(\alpha;\gamma;z) \backsim (-1)^\gamma \frac{\Gamma(\gamma)}{\Gamma(\gamma-\alpha)} z^{-\alpha} \sum_{n=0}^{\infty} \frac{\Gamma(n+\alpha)\,\Gamma(n+\alpha-\gamma+1)(-1)^n}{\Gamma(\alpha)\,\Gamma(\alpha-\gamma+1)\,n!\,z^n}. \tag{25}$$

The form of equation (25) suggests the possibility of finding a second integral expression for $W_s(\alpha;\gamma;z)$. This arises from the fact that the quantity

$$\frac{\Gamma(n+\alpha)\,\Gamma(n+\alpha-\gamma+1)(-1)^n}{\underline{n}\,z^n}$$

is the residue of

$$\Gamma(s)\,\Gamma(-s+\alpha)\,\Gamma(-s+\alpha-\gamma+1)z^s = f(s)$$

at the simple poles $s = -n$ $(n = 0,1,2,\ldots.)$. Consequently, it is possible to express W_s as

$$W_s(\alpha;\gamma;z) = (-1)^\gamma \frac{\Gamma(\gamma)}{\Gamma(\gamma-\alpha)} \frac{z^{-\alpha}}{2\pi i} 2\pi i \sum_{n=0}^{\infty} R_{s=-n},$$

where $R_{s=-n}$ is the residue of $f(s)$ at the simple pole $s = -n$. Thus, it seems reasonable to write

$$W_s(\alpha;\gamma;z) = (-1)^\gamma \frac{\Gamma(\gamma)}{\Gamma(\gamma-\alpha)} \frac{z^{-\alpha}}{2\pi i} \int_{C_i} \frac{\Gamma(s)\,\Gamma(-s+\alpha)\,\Gamma(-s+\alpha-\gamma+1)z^s ds}{\Gamma(\alpha)\,\Gamma(\alpha-\gamma+1)} \tag{26}$$

where the contour, C_i, is one which encloses the simple poles $s = -n$ $(n = 0,1,2,\ldots.)$ of $f(s)$ but excludes all the others. It can be shown[4] that the contour, C_i, may be taken to consist of the imaginary axis from $-\infty i$ to $+\infty i$ with loops if necessary to keep the poles, $s = -n$, to the left of the path and all others to the right of the path.

That $W_s(\alpha;\gamma;z)$ as expressed in equation (26) is a solution of equation (18) can be proved by direct substitution in that equation. That it is the analytical continuation of $W_s(\alpha;\gamma;z)$ as expressed in equation (24) can also be proved.[4]

The asymptotic expansion of $W_s(\alpha;\gamma;z)$ has been found. It is now necessary to find the expansion valid for all values of z. This may be obtained as follows. If we take the expression

$$\Gamma(s)\,\Gamma(-s+\alpha)\,\Gamma(-s+\alpha-\gamma+1) = \Theta(s),$$

and carry out the integration

$$\int \Theta(s) z^s\, ds$$

taken around a semi-circle on the right of the imaginary axis, it can be shown[4] that the integral tends toward zero as the radius of the circle tends toward infinity. Thus we may write

$$W_s(\alpha;\gamma;z) = (-1)^{\gamma+1} \frac{\Gamma(\gamma)}{\Gamma(\gamma-\alpha)\,\Gamma(\alpha)\,\Gamma(\alpha-\gamma+1)} z^{-\alpha}(\Sigma R'), \tag{27}$$

where $(\Sigma R')$ denotes the sum of the residues of $f(s)$ on the right of the contour, C_i.

In FIGURE 2 the poles of $f(s)$ are indicated. The part, $\Gamma(-s+\alpha-\gamma+1)$, has simple poles at $s = \alpha-\gamma+1+n$ $(n = 0, 1\ldots.)$, and the part, $\Gamma(-s+\alpha)$, has simple poles at $s = \alpha+n$, $(n = 0, 1,\ldots.)$. Thus, there are both simple and double poles on the right hand side of the path of integration. Consequently $(\Sigma R')$ may be written as

$$(\Sigma R') = \sum_{n=0}^{\gamma-2} R'_{s=\alpha-\gamma+1+n} + \sum_{n=0}^{\infty} R''_{s=\alpha+n}, \tag{28}$$

where $R'_{s=\alpha-\gamma+1+n}$ denotes the residue of $f(s)$ at the simple pole, $s = \alpha-\gamma+1+n$, and $R''_{s=\alpha+n}$ denotes the residue of $f(s)$ at the double pole, $s = \alpha+n$.

From the properties of the Γ functions it is evident that

$$R'_{s=\alpha-\gamma+1+n} = \frac{\Gamma(n+\alpha-\gamma+1)\,\Gamma(\gamma-n-1)(-1)^{n+1} z^{n+\alpha-\gamma+1}}{n!}. \tag{29}$$

To evaluate $R''_{s=\alpha+n}$, we proceed as follows: using the relation

$$\Gamma(x)\,\Gamma(1-x) = \frac{\pi}{\sin \pi x}$$

we may express $f(s)$ as

$$f(s) = \frac{\pi^2}{(-1)^{\gamma+1}\sin^2\pi(s-\alpha)}\,\phi(s),$$

where

$$\phi(s) = \frac{\Gamma(s)z^s}{\Gamma(1-\alpha+s)\,\Gamma(\gamma-\alpha+s)}.$$

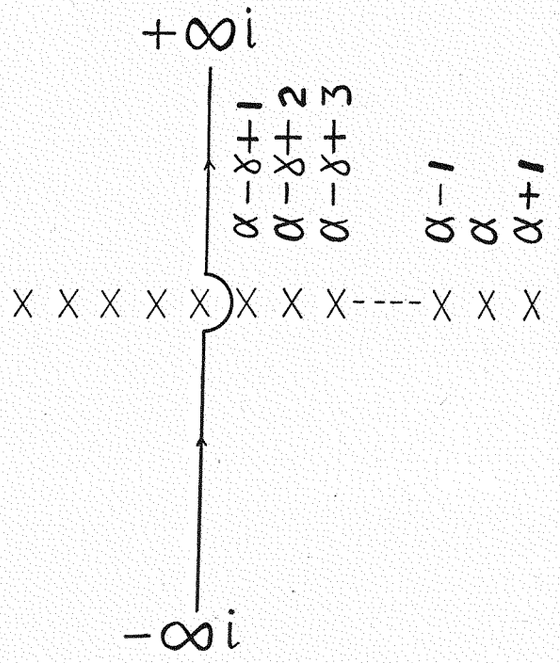

FIGURE 2

Now, utilizing the well known relation

$$\frac{\pi^2}{\sin^2\pi(s-\alpha)} = \sum_{n=-\infty}^{\infty}\left[\frac{1}{(s-\alpha-n)^2}\right],$$

and the Taylor expansion of $\phi(s)$ about the point, $s = \alpha + n$, we get for $f(s)$ the following;

$$f(s) = \ldots\ldots \frac{(-1)^{-\gamma-1}}{(s-\alpha-n)^2}\{\phi(s)_{s=\alpha+n} + (s-\alpha-n)\phi'(s)_{s=\alpha+n} + \ldots\ldots\} + \ldots\ldots,$$

from which it is evident that the residue of $f(s)$ at the double pole, $s = \alpha + n$, is

$$(-1)^{-\gamma-1}\,\phi'(s)_{\sigma=\alpha+n}. \qquad (30)$$

Writing $s = \sigma + n$, we have

$$\phi'(s)_{s=\alpha+n} = \frac{d}{d\sigma}\left[\frac{\Gamma(\sigma+\alpha)z^{\sigma+\alpha}}{\Gamma(\sigma+1)\,\Gamma(\sigma+\gamma)}\right]_{\sigma=n}.$$

The expression on the right of the above equation can easily be evaluated with the help of the following relations[5]

$$\left[\frac{d}{d\sigma}\Gamma(\sigma+\alpha)\right]_{\sigma=n} = \Gamma(n+\alpha)\left\{\frac{1}{\alpha} + \frac{1}{\alpha+1} + \ldots\ldots + \frac{1}{\alpha+n-1} + \frac{\Gamma'(\alpha)}{\Gamma(\alpha)}\right\}, \quad \frac{\Gamma'(1)}{\Gamma(1)} = -C,$$

where C, Euler's constant, $= .5772\ldots\ldots$ Carrying through the differentiation one finds

$$\phi'(s)_{s=\alpha+n} = \frac{\Gamma(\alpha)}{\Gamma(\gamma)}\,D_n z^{\alpha+n}\{\ln z + B_n + \Psi(\alpha) - \Psi(\gamma) + C\}, \qquad (31)$$

where

$$D_n = \frac{\Gamma(n+\alpha)\,\Gamma(\gamma)}{\Gamma(\alpha)\,\Gamma(n+\gamma)}\,\frac{1}{n!},$$

$$B_n = \left(\frac{1}{\alpha} + \frac{1}{\alpha+1} + \ldots\ldots + \frac{1}{\alpha+n-1}\right) - \left(\frac{1}{\gamma} + \frac{1}{\gamma+1} + \ldots\ldots + \frac{1}{\gamma+n-1}\right) - \left(1 + \frac{1}{2} + \ldots\ldots + \frac{1}{n}\right),$$

$B_0 = 0$, and $\Psi(\alpha) = \Gamma'(\alpha)/\Gamma(\alpha)$.

Extensive tables of the Ψ function are available.[6]

We are now in a position to write down the complete expression for $W_s(\alpha;\gamma;z)$; *viz.*, (cf. equations 27 to 31)

$$W_s(\alpha;\gamma;z) = \frac{\sin\pi\alpha}{\pi}\left[(-1)^{\gamma+1}F(\alpha;\gamma;z)\{\ln z + \Psi(\alpha) - \Psi(\gamma) + C\} + \sum_{n=0}^{\gamma-2}\frac{\Gamma(\gamma)\,\Gamma(n+\alpha-\gamma+1)\,\Gamma(\gamma-n-1)\,(-1)^{n+1}}{\Gamma(\alpha)n!\,z^{\gamma-n-1}} + (-1)^{\gamma+1}\sum_{n=1}^{\infty}D_nB_nz^n\right]. \qquad (32)$$

This gives a second solution of equation (18) in a form that could be used for computations. However, a solution with more convenient properties is the following:

$$W(\alpha;\gamma;z) = (-1)^{\gamma+1}\left[\frac{\pi}{\sin\pi\alpha}\,W_s(\alpha;\gamma;z) + (-1)^{\gamma+1}\,\pi\cot\pi\alpha\,F(\alpha;\gamma;z)\right], \qquad (33)$$

[5] **Courant, R., & Hilbert, D.** "Methoden der Mathematischen Physik." Vol. I. Springer. Berlin. 1924. p. 406.

[6] **Davis, H. T.** "Tables of Higher Mathematical Functions." Vol. I. The Principia Press. Bloomington, Ind. 1933.

or

$$W(\alpha;\gamma;z) = -i\pi\, W_1(\alpha;\gamma;z) + \pi \cot \pi\alpha\, W_2(\alpha;\gamma;z). \tag{34}$$

[From equations (34) and (23a) (23b), one gets the asymptotic expansion of $W(\alpha;\gamma;z)$.]

From equations (32) and (33) and the relation

$$\Psi(1-\alpha) = \Psi(\alpha) + \pi \cot \pi\alpha,$$

we have

$$W(\alpha;\gamma;z) = F(\alpha;\gamma;z)\{\ln z + \Psi(1-\alpha) - \Psi(\gamma) + C\} + (-1)^{\gamma} \sum_{n=0}^{\gamma-2} \frac{\Gamma(\gamma)\,\Gamma(n+\alpha-\gamma+1)\,\Gamma(\gamma-n-1)\,(-1)^n}{\Gamma(\alpha)\,n!\,z^{\gamma-n-1}} + \sum_{n=1}^{\infty} D_n B_n z^n. \tag{35}$$

The reason that $W(\alpha;\gamma;z)$ as expressed in equation (35) has been chosen from all the many possible solutions is that it shares with $F(\alpha;\gamma;z)$ the following properties which are very useful when one tries to make computations:

$$\frac{d}{dz} F(\alpha;\gamma;z) = \frac{\alpha}{\gamma} F(\alpha+1;\gamma+1;z), \tag{36}$$

$$\alpha F(\alpha+1;\gamma+1;z) = (\alpha-\gamma)\, F(\alpha;\gamma+1;z) + \gamma F(\alpha;\gamma;z), \tag{37}$$

$$\alpha F(\alpha+1;\gamma;z) = (z+2\alpha-\gamma)\, F(\alpha;\gamma;z) + (\gamma-\alpha)\, F(\alpha-1;\gamma;z). \tag{38}$$

IV

We have now found two independent solutions of equation (7), *viz*, $F(\alpha;1;z)$ and $W(\alpha;1;z)$. Thus, everything necessary for making computations from equation (17) is known. However, some of the expressions in the formal treatment can be more simply expressed, now that some of the properties of the functions used are known. For example, the determinant (12) can be simplified; with the help of equations (36) and (37) it becomes

$$(\alpha-1) \begin{vmatrix} F(\alpha;2;a), & W(\alpha;2;a) \\ F(\alpha;2;b), & W(\alpha;2;b) \end{vmatrix} = 0. \tag{39}$$

Thus the permissible values of α are the roots of equation (39). It is obvious that the root $\alpha_0 = 1$ has a particular significance. From equation (17) one sees that the term in the expression for $c(z,t)$ for which $\alpha_0 = 1$ is independent of the time, *i.e.*, this term gives $c(z,\infty)$, or the distribution of concentration when equilibrium has been reached.

A further aid to computation would be to get rid of the integrals in equation (17). Both of these integrals can be evaluated but in the case of the one in the denominator no simplification results from doing so.

The integral in the numerator can be evaluated in the following manner. Let

$$M_{\alpha_n}(z) = e^z\, S_{\alpha_n}(z).$$

Then S_{α_n} is found to be a solution of

$$z\, S''_{\alpha_n} + (1+z)\, S'_{\alpha_n} - (\alpha_n - 1)\, S_{\alpha_n} = 0, \tag{40}$$

where the superscripts denote differentiation with respect to z. Thus, from equation (40)

$$(\alpha_n - 1)\int S_{\alpha_n} dz = \int (zS''_{\alpha_n} + S'_{\alpha_n})dz + \int zS'_{\alpha_n} dz = z(S'_{\alpha_n} + S_{\alpha_n}) - \int S_{\alpha_n} dz.$$

Therefore,

$$\int S_{\alpha_n} dz = \frac{z}{\alpha_n}(S'_{\alpha_n} + S_{\alpha_n}),$$

or,

$$\int_a^b e^{-z}\, M_{\alpha_n} dz = \frac{b}{\alpha_n} e^{-b}\, M_{\alpha_n}(b) - \frac{a}{\alpha_n} e^{-a}\, M_{\alpha_n}(a), \tag{41}$$

since $M'_{\alpha_n}(z) = M_{\alpha_n}(z)$ for $z = (a,b)$.

Thus, equation (17) may be written as follows:

$$\frac{c}{c_0} = \sum_{n=0}^{\infty} \left[\frac{be^{-b}M(\alpha_n;1;b) - ae^{-a}M(\alpha_n;1;a)}{\alpha_n \int_a^b e^{-z}\{M(\alpha_n;1;z)\}^2 dz}\, M(\alpha_n;1;z) e^{(\alpha_n-1)\tau} \right] = \sum_{n=0}^{\infty} T_{\alpha_n}, \tag{42}$$

where

$$M(\alpha_n;1;z) = F(\alpha_n;1;z) - \frac{F(\alpha_n;2;a)}{W(\alpha_n;2;b)}\, W(\alpha_n;1;z). \tag{43}$$

The term for which $\alpha_0 = 1$ can be greatly simplified. We have

$$M(1;1;z) = e^z,$$

since $W(1;2;a) = \infty$ and $F(1;1;z) = e^z$. Thus we may write equation (42) in the form

$$\frac{c}{c_0} = \frac{b-a}{e^b - e^a} e^z + \sum_{n=1}^{\infty} T_{\alpha_n}, \tag{44}$$

where the values of α_n are the roots of the equation

$$F(\alpha;2;a)\, W(\alpha;2;b) - F(\alpha;2;b)\, W(\alpha;2;a) = 0. \tag{45}$$

Let us now use equation (44) to calculate c/c_0 for an actual experiment for different values of $\tau(=2\omega^2 st)$. We will plot c/c_0 as a function of z, where

$$z = \frac{\omega^2 s}{2D} r^2 = \frac{M(1 - V\rho)\omega^2}{2RT} r^2.$$

(The proof of the relation $\frac{s}{D} = \frac{M(1 - V\rho)}{RT}$ is to be found in many places in the literature.) In these expressions M is the molecular weight, V the partial specific volume of the dissolved substance, and ρ the density of the solution.

The computations will be made for an actual experiment described by Svedberg,[7] in which the dissolved substance was carbon-monoxide hemoglobin which has a molecular weight, $M = 68{,}000$, and a partial specific volume, $V = 0.749$ cm.^{3}/gm. For the cell used $r_1 = 4.16$ cm. and $r_2 = 4.61$ cm. Also $\omega = 290\pi$ and $T = 293°$ K. These data are sufficient to determine the two constants, a and b. We have

$$\begin{Bmatrix} a \\ b \end{Bmatrix} = \frac{M(1 - V\rho)\omega^2}{2RT} \begin{Bmatrix} r_1^2 \\ r_2^2 \end{Bmatrix}.$$

The numerical values are $a = 5.0$ and $b = 6.2$.

The first task is that of finding the roots of equation (45). This involves the computation of the expressions $F(\alpha;2;5.0)$, $F(\alpha;2;6.2)$, $W(\alpha;2;5.0)$ and $W(\alpha;2;6.2)$ as functions of α. (The recurrence formulae (37) and (38) are very useful for this purpose.) These particular functions have been calculated for values of α between 2.0 and -41.0 at intervals of 0.2. The next step is to combine them to form the function

$$y = F(\alpha;2;5)\, W(\alpha;2;6.2) - F(\alpha;2;6.2)\, W(\alpha;2;5) = f(\alpha). \quad (46)$$

The quantity, $y = f(\alpha)$, becomes zero for a series of values of α which are infinite in number. The first one is $\alpha_1 = -38.7$, and all the others have much larger negative values; the others have such large negative values that the terms in equation (42) for which $n = 2$ are relatively unimportant in comparison with the first two terms with $n = 0$ and 1.

Consequently, if only the first two terms of equation (44) are used we have

$$\frac{c}{c_0} = .003485e^z + \frac{6.2e^{-6.2}\, M(-38.7;1;6.2) - 5e^{-5}\, M(-38.7;1;5)}{(-38.7)\int_{5.0}^{6.2} e^{-z}\{M(-38.7;1;z)\}^2 dz}\, M(-38.7;1;z)e^{-39.7\tau}. \quad (47)$$

[7] **Svedberg, T.** in "Colloidal Chemistry, Theoretical and Applied." J. Alexander, ed. Chemica Catalog Co. New York. 1926.

TABLE 1 gives the values of $M(-38.7;1;z)$ for z between 5.0 and 6.2.

TABLE 1

z	$M\ (-38.7;1;z)$
5.0	−3.4526
5.1	−3.6820
5.2	−3.6215
5.3	−3.3101
5.4	−2.6768
5.5	−1.7874
5.6	−0.7095
5.7	+0.4885
5.8	+1.7500
5.9	+3.0005
6.0	+4.1777
6.1	+5.1849
6.2	+5.9504

The integral in equation (47) was evaluated several ways and was found to have the value .04707. Combining these results, equation (47) reduces to

$$\frac{c}{c_0} = .003485e^z - .1050\, M(-38.7;1;z)e^{-39.7\tau} + \ldots. \quad (48)$$

TABLE 2

c/c_0 AS A FUNCTION OF z, FROM EQUATION (48) WHEN $\tau\ (= 2\omega^2 st)$ IS ZERO.

z	c/c_0
5.0	.880
5.2	1.012
5.4	1.053
5.6	1.017
5.8	.968
6.0	.968
6.2	1.093

It is interesting to evaluate equation (48) for the case $\tau = 0$ for then c/c_0 should equal unity for all values of z between 5.0 and 6.2. TABLE 2 contains the values of c/c_0 for $\tau = 0$. Except at the very end of the range, c/c_0 is equal to unity to within 4 or 5 per cent. Thus, the contribution of the higher terms of equation (44) to $c(z,t)$ are small compared with that of the first two. In addition, the case in which $\tau = 0$ is the most unfavourable one. Even when τ has a very small value (say $\tau = .01$) these higher terms become much less important because of the large values of α. Because of these considerations, as well as the knowl-

TABLE 3

$c\ (z, \tau)$ AS CALCULATED FROM EQUATION (48)

z	$\tau = .015$	$\tau = .03$	$\tau = .05$	$\tau = .1$	$\tau = \infty$
5.0	.717	.627	.567	.524	.517
5.1	.784	.689	.625		.572
5.2	.841	.747	.684	.639	.632
5.3	.889	.804	.746		.698
5.4	.926	.857	.810	.777	.772
5.5	.956	.910	.879		.853
5.6	.983	.965	.953	.944	.942
5.7	1.013	1.026	1.035		1.042
5.8	1.050	1.095	1.126	1.148	1.151
5.9	1.099	1.177	1.229		1.272
6.0	1.165	1.273	1.346	1.398	1.406
6.1	1.254	1.389	1.479		1.554
6.2	1.374	1.528	1.632	1.705	1.717

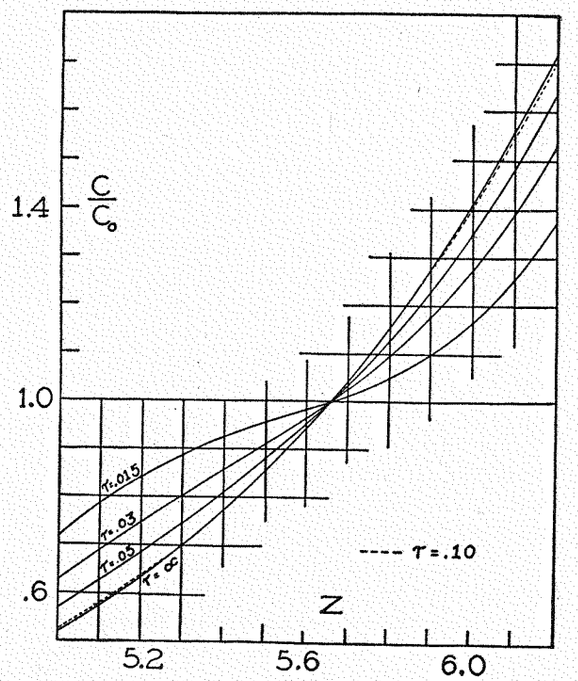

FIGURE 3. Values of concentration change c/c_0 (c_0 = initial constant concentration) as a function of position z ($= \omega^2 s t^2/2D$) for various values of τ ($= 2\omega^2 s t$) when $a = 5.0$ and $b = 6.2$.

edge of the properties of the functions obtained from working with them, it is felt that the curves obtained are accurate. However, one would prefer to calculate at least one more term of the series but the labour involved seemed prohibitive.

The values of $c(z,t)$ are recorded in TABLE 3 for different values of z and τ and are plotted in FIGURE 3. The calculations show that the concentration has practically reached equilibrium when $\tau(= 2\omega^2 s t)$ has the value 0.10. Since $s \backsim 5 \times 10^{-13}$ for carbon-monoxide hemoglobin, this corresponds to a time of 33 hours. In the actual experiment an exponential distribution of concentration had been reached after a period of 39 hours.

THE PRESENT STATUS OF MOLECULAR WEIGHTS OF PROTEINS

By Alexandre Rothen

From the Laboratories of The Rockefeller Institute for Medical Research, New York

Seventeen years have elapsed since Svedberg and Fåhraeus made the first determination of molecular weight of a protein by ultracentrifugation. Since that time, work in this field has been extensive in this country as well as abroad, and a considerable amount of data has been accumulated. Now seems a good time to survey the whole situation; to discuss the method and to find out in which direction lies progress.

Starting from the position of two years ago when Svedberg's book was published, we shall see what have been the recent developments since the chapter on proteins by Pedersen was written. First we shall briefly review the limitation of the method and discuss what possible improvements in the technique could be made; then we shall review some of the results obtained in the last two years; and finally speculate on the future of the ultracentrifuge.

The most popular method for the calculation of molecular weights of proteins still is the determination of the rate of sedimentation and of the diffusion constant. The Svedberg formula

$$M = \frac{s\,RT}{D(1 - V\rho)}$$

has been so often used that it can be regarded as classic. It seems that in the future the definition of the different constants could be omitted when using this equation. It is the general practice to give the value of s in C.G.S. units and to add words such as: sedimentation constants are given in centimeters per second per dyne. Such a statement is incorrect, because it is per unit of field and not per dyne. If necessary it would be shorter to say "in seconds," since the constant of sedimentation has the dimension of time.

One reason for the popularity of this method is the relatively short time necessary for the determination. Another is that the method is much more sensitive as a test of homogeneity than the equilibrium method.

In the past, diffusion constants were very often not determined at all or they were estimated from the spreading of the boundary observed in

the centrifuge. It is a welcome improvement that in most of the recent investigations on molecular weights of proteins, the diffusion constant was independently determined. The diffusion constant is determined optically mainly by a modification of the schlieren method with a precision of about 1 per cent. It might be said *en passant* that more than 30 years ago, Thovert in France employed very successfully an optical device based on the use of an inclined slit and of a cylindrical lens for the determination of diffusion constants, and the curves he published were excellent.

The precision obtained in a determination of the rate of sedimentation is practically independent of the optical method used for observing the moving boundary. The method most commonly employed is the so-called "schlieren" method which has superseded in the last two years the accurate but time-consuming method of Lamm. The schlieren method, whether used in the form of the Longsworth scanning device or in the form of the Thovert-Philpot modification, permits a rapid evaluation of a rate of sedimentation. It is fair to say that the error in the calculation of a rate of sedimentation of a protein whose molecular weight is not too small (let us say not smaller than 30,000) is less than 1 per cent, the error in the speed of rotation term ω^2 being negligible (less than 0.1 per cent). The usual correction formula

$$s_{20}^0 = s_t \frac{\eta_t}{\eta_{20}^0} \frac{1 - V_{20}\rho_{20}^0}{1 - V_t\rho_t}$$

has proved satisfactory. Obviously the temperature must be known at least within 0.4°C. if the error in the viscosity is not to exceed the maximum error in estimating s_t.

It is the difficulty of maintaining the temperature constant over a long interval of time which seems nowadays to be the limiting factor in the accuracy of the determination of the rate of sedimentation of a small protein molecule. This difficulty does not exist for speeds lower than 40,000 r.p.m.

Recently, at the suggestion of Dr. MacInnes, we installed in our air-driven centrifuge a cooling coil connected with a Frigidaire unit. This was to have a double purpose: first, to make possible experiments at low temperatures; and second, to exert a better control on the temperature of the rotor. It also seems desirable to determine the physical properties of proteins at 0°C. By adding hydrogen at low pressure (about 0.1 mm. Hg), it was found that the temperature of the rotor could be kept for 5 to 6 hours easily within the small range of 1°C. when the rotation was 57,600 r.p.m. By carefully adjusting the temperature of the chamber somewhat lower than that of the rotor, the heating of the rotor by the residual air and hydrogen can be exactly compensated by the cooling due to the coil. There is no doubt that with some care the constancy of the rotor could be maintained within ± 0.1°C. at the highest velocity. A few experiments at temperatures as low as 2° to 3°C. were found satisfactory.

To test the accuracy of the rates of sedimentation, Stanley and Lauffer[1] had the excellent idea of having some determinations made in five different laboratories on samples of the same preparation of bushy stunt virus. Besides the laboratories of the Princeton branch of the Rockefeller Institute, determinations were made in the laboratories of Dr. J. W. Williams of the University of Wisconsin, Dr. J. W. Beard of Duke University, Dr. A. S. McFarlane of the Lister Institute in London, and our own laboratory at the Rockefeller Institute in New York. The choice of bushy stunt virus was an excellent one, since its large size and its homogeneity made the conditions for accuracy as good as possible. The results are interesting. It might have been predicted that the results should have agreed within 1 per cent. As a matter of fact, differences as large as 10 per cent occurred. However, variations of the same order of magnitude were observed in a series of determinations made in the same laboratory by the same worker. Lauffer[2] calculated a probable error of 1.9×10^{-13} for the sedimentation constant of bushy stunt virus, $s_{20}^0 = 132.0 \times 10^{-13}$. It can then be concluded that under the best experimental conditions, variations of a few per cent occurred in successive determinations of the rate of sedimentation of bushy stunt virus. These variations are larger than those expected from the known causes of error. It remains to be seen whether some unsuspected cause of error is responsible for such discrepancies or whether these variations represent something happening to the average size or shape of the virus.

SPECIFIC VOLUME

The most uncertain constant in the molecular weight determination by ultracentrifugation is still the true value for the specific volume of a protein. Generally, the specific volume is determined by measuring the density of a solution of known concentration. However, in a few cases the specific volume was assumed to be equal to the reciprocal value of the density of the solution in which no sedimentation occurred. This method was first suggested by McBain[3] and was applied by Smadel, Pickels, and

[1] **Stanley, W. M., & Lauffer, M. A.** Jour. Biol. Chem. **135**: 463. 1940.
[2] **Lauffer, M. A.** Jour. Phys. Chem. **44**: 1137. 1940.
[3] **McBain, J. W.** Jour. Amer. Chem. Soc. **58**: 315. 1936.

Shedlovsky[4] in the case of vaccine virus. The disadvantages of this method are: first, one does not know whether the substance added to increase the density of the solution does not react with or alter the protein; second, if the molecule is hydrated, the specific volume thus measured corresponds to the hydrated form and the molecular weight calculated corresponds also to the hydrated form; third, the method is impractical for small proteins for which the rate of sedimentation is low.

The specific volume found for most proteins is about 0.75, although some proteins have a density considerably higher than this average value. For instance, ribonuclease[5] has a specific volume of 0.71 and calf thymus nucleohistone[6] has a reported value as low as 0.66. It should be of interest to know why these proteins have such high densities, and whether it is due to the presence of heavy metals or some bound electrolytes. It is a matter of experience that the density of a crystalline protein in the solid phase is smaller than the density obtained in solution, this difference being due to the presence of water of crystallization.

Some of the results obtained by Adair and Adair[7] have been summarized in TABLE 1. They indicate the order of magnitude of the differences between the density of the crystals and the density of the protein in solution as well as the amount of hydration which can be estimated from such measurements.

TABLE 1
PARTIAL SPECIFIC VOLUMES OF PROTEINS IN AQUEOUS SOLUTIONS AND IN CRYSTALLINE FORM

Substance	Aqueous solution V	Aqueous solution δ	Crystals δ	Hydration %
Sheep hemoglobin	0.752	1.329	1.260	17
Horse serum albumin	0.742	1.348	1.280	20
Egg albumin	0.746	1.341	1.260	20
Edestin	0.744	1.346	1.290	14

These figures indicate an order of magnitude, since the density of the crystals depends somewhat on the medium in which they are suspended. But the question remains open: To what extent is the protein molecule hydrated in solution? From which follows the second question: If hydrated, how is the molecular weight affected when determined by ultracentrifugation? This problem has been treated by Kraemer[8] and the following equation obtained:

[4] **Smadel, J. E., Pickels, E. G., & Shedlovsky, T.** Jour. Exp. Med. **68**: 607. 1938.
[5] **Rothen, A.** Jour. Gen. Physiol. **24**: 203. 1940-41.
[6] **Carter, R. O.** Jour. Amer. Chem. Soc. **63**: 1960. 1941.
[7] **Adair, G. S. & Adair, M. E.** Proc. Roy. Soc. **B 120**: 422. 1936
[8] **Kraemer, E. O.** Jour. Franklin Inst. **229**: 393, 531. 1940.

$$M_1 = M_1^a \frac{(1 - V_1)}{(1 - V_1\rho) + \Sigma r_i(1 - V_i\rho)}.$$

This equation can be transformed in the case of a binary solution into

$$M_1 = M_1^a \frac{1 - m_1}{1 - m_1 - rm_1}.$$

M_1 = true molecular weight of the unhydrated molecule
M_1^a = apparent molecular weight as determined in the centrifuge
V_1 = partial specific volume of protein
ρ = density of medium
r_1 = grams of component i combined with 1 gm. of component M_1
m_1 = weight fraction concentration of component M_1 without solvent
r = grams of solvent combined with 1 gm. of component M_1.

Since m_1 is small and rm_1 still smaller, it is apparent from the above equation that the value for M obtained in the ultracentrifuge is practically the same as the value for the unhydrated molecule, or rather for the molecule whose specific volume was determined by density measurements. As pointed out by Kraemer, in the case of a protein dissolved in buffer solutions, such as those used for centrifugation, a hydration of 25 per cent would lead to a molecular weight only 1 per cent lower than the molecular weight of the unhydrated molecule. This result can be understood if one realizes that in case of a binary solution, hydration affects the sedimentation and the diffusion constants in the same way. Both constants decrease linearly with the increase due to hydration of the diameter of the molecule, provided the density of the bound water is the same as that of the free water. But the molecular weight will be affected by hydration if the specific volume of the protein is determined by measuring the density of the medium in which no sedimentation occurs. Theoretically at least, a comparison of the specific volume arrived at by the two methods should indicate whether the protein is hydrated or not. However, as mentioned by Kraemer,[8] the difficulty is to find an inert material which will bring the density of the medium equal to that of the protein without combining with the protein or reducing the solvation if it exists. Electrolytes are excluded, but carbohydrates might be tried. It seems that efforts should be made in that direction if the question of hydration of proteins is ever to be solved.

EQUILIBRIUM METHOD

The number of investigations making use of the distribution of the particles at equilibrium has been small, undoubtedly on account of the

time involved in such measurements. The scale method usually has been employed and the molecular weight calculated by the formula,

$$M = \frac{2RT \log (Z_2 x_1 / Z_1 x_2)}{(x_2^2 - x_1^2)(1 - V\rho)},$$

Z_1 and Z_2 being the scale displacements observed at distances x_1 and x_2.

The equilibrium method must be used when systems containing molecules smaller than 10,000 are investigated.

Since the integration of the differential equation for the combined sedimentation and diffusion has been solved by Archibald, it would be of interest to discuss its possible application to the determination of molecular weights of proteins. Tables could be prepared using his results, from which it should be possible to calculate the molecular weight before equilibrium is established and also to predict how long it will take to reach equilibrium.

THE SHAPE FACTOR f/f_0

As can be gathered from the most recent articles on the subject, our knowledge on the interpretation of the asymmetry factor has not advanced much since the excellent review presented by Oncley[9] at the New York Academy of Sciences. The statement that the factor is a measure of the asymmetry or of the hydration of the protein, or most probably a combination of both factors can still be found in all publications on this question. It has been the tendency, however, to neglect the contribution of hydration in estimating the shape of the protein molecules.[10]

Great advance would be made if one could study separately the two factors, f/f_e and f_e/f_0, into which the observed frictional ratio, $f/f_0 = f/f_e \cdot f_e/f_0$ can be broken; f/f_e represents the hydration factor and f_e/f_0 the asymmetry factor. A fair knowledge of the specific volume of the hydrated molecule would permit us to calculate separately the factors,

$$\frac{f_e}{f_0} \cdot \frac{f}{f_e} = \left(\frac{V_1 + rV_2}{V_1}\right)^{\frac{1}{3}},$$

where r is the number of grams of water combined with 1 gm. of protein.

Assuming that the shape of a protein molecule can be approximated by an ellipsoid of revolution, the axis of such an oblong or oblate ellipsoid has often been calculated with the use of the formula of Perrin.

Many authors have assumed that protein molecules are oblong rather than oblate. This was often unjustified. Data obtained with the aid

[9] **Oncley, J. L.** Ann. N. Y. Acad. Sci. **41**: 121. 1941.
[10] **Neurath, H.** Jour. Amer. Chem. Soc. **61**: 1841. 1939.

of the centrifuge cannot permit a differentiation between the two types of shape. When double refraction of flow can be observed, it is theoretically possible to distinguish between rod shape or disc shape. If in the case of disc-like particles the birefringence is due mostly to the orientation effect, then it should disappear at right angles to the direction of flow in a small capillary[11].

RECENT MOLECULAR WEIGHT DETERMINATIONS OF PROTEINS

Since the publication of Svedberg's table a few new proteins have been investigated in the ultracentrifuge. Ribonuclease, the enzyme depolymerizing ribonucleic acid was crystallized by Kunitz.[12] The material was beautifully crystalline. We studied this crystalline material in the ultracentrifuge. It proved homogeneous and the molecular weight arrived at by sedimentation and diffusion was 12,700. In this calculation the variation in the density of water with the hydrostatic pressure was not corrected for. When the correction is applied a value of about 13,000 is found for the molecular weight. The value obtained by equilibrium measurements was 13,000 and the frictional ratio was $f/f_0 = 1.04$, showing that this small protein molecule was highly symmetric.

Fankuchen,[13] who made an X-ray study of this material, derived a maximum molecular weight of 15,700 $\pm$ 300 from the dimensions of the unit cell (77,300 A^3 with 4 molecules per unit) and the density of the crystal ($\vartheta = 1.341$ by flotation). Now, as mentioned above, the molecular weight obtained by centrifugation is within a few per cent the weight of the unsolvated molecule, with a specific volume in this case of 0.709 as compared to 0.746 for the crystal. The difference between these two values is of the same order of magnitude as that found for other proteins (see TABLE 1). From it, the hydration of the crystal can be estimated to be about 13 per cent from which follows a value of 13,700 $\pm$ 300 for the unhydrated molecule of ribonuclease. It can then be concluded that the agreement between the two methods is satisfactory.

Another small protein[14] submitted recently to ultracentrifuge analysis is the active oxytocic-pressor hormone from the posterior lobe of the pituitary gland (protein of the *pars neuralis* of the ox). This protein was found to be homogeneous in the ultracentrifuge as well as from

[11] **Lauffer, M. A.** Cold Spring Harbor Symposium on Quantitative Biology **6**: 227. 1938.
[12] **Kunitz, M.** Jour. Gen. Physiol. **24**: 15. 1940–41.
[13] **Fankuchen, I.** Jour. Gen. Physiol. **24**: 315. 1940–41.
[14] **Van Dyke, H. B., Chow, B. F., Greep, R. O. & Rothen, A.** Amer. Jour. Physiol. **133**: 473. 1941.

solubility tests. Its solubility curve was as good as that found for the best crystalline proteins. The sedimentation constant $s_{20}^0 = 2.6 \times 10^{-13}$ to 2.8×10^{-13}, in conjunction with a diffusion constant of $D_{20} = 8.5 \times 10^{-7}$, led to a molecular weight of 30,000. Similar studies were carried out with metakentrin,[15] a luteinizing hormone of the anterior lobe. Tests for homogeneity were satisfactory and an approximate molecular weight of 90,000 was found (work is in progress to obtain a more precise value).

In conjunction with these studies a discussion of the so-called "Svedberg unit" seems appropriate. From the chapter by Pedersen in Svedberg's book it would seem a well proven fact that molecular weights of proteins are simple multiples of a single unit of a weight of about 17,600, the deviations which occur being simply explained by the distribution of smaller or larger amino acids in the units.

Several speculations from different quarters have been advanced for the explanation of such facts. (See for instance the work of Astbury and Woods, Bergmann and Niemann, and of Wrinch.) In our opinion the argument of Pedersen is based on insufficient evidence to prove definitely the reality of the unit. As we have seen, an error as great as 8 per cent in the molecular weight of a protein determined by centrifugal methods can very well occur. It follows that all proteins with a molecular weight greater than 100,000 are unsuitable materials to test the hypothesis of the Svedberg unit, since the experimental error amounts to 50 per cent of the unit and any number greater than 100,000 could be looked at as a multiple of the unit within experimental error. In other words, it is not justified to explain molecular weights greater than 100,000 as multiples of 17,600 as is done in the tabulation of Pedersen. Let us see what is the evidence for molecular weights smaller than 100,000. Pedersen reports 23 proteins with a molecular weight smaller than 100,000 (see TABLE 2). Five of them with molecular weights varying from 15,600 to 18,000 have served as the basis for the unit. Thirteen proteins are given to fit into the pattern $2 \times 17,600 = 35,200$, but there are serious discrepancies. One molecular weight (crotoxin) is as low as 30,000, 5 proteins are in the range 40,000 (zein) to 44,000 (ovalbumin) of which 3 could fit just as well into the scheme $3 \times 17,600$. In other words, 50 per cent of the examples disprove rather than prove the rule.

Four proteins are given as evidence for the combination $4 \times 17,600 = 70,400$. Out of these four, human hemoglobin falls midway between

[15] **Shedlovsky, T., Rothen, A., Greep, R. O., van Dyke, H. B., & Chow, B. F.** Science **92**: 178. 1940.

TABLE 2
MOLECULAR CONSTANTS OF PROTEINS

Protein	M_s	M_e
Erythrocruorin (Lampetra)	17,100	19,100
Lactalbumin	17,400	—
Cytochrome	15,600	—
Myoglobin	16,900	17,500
Bacillus Phlei Protein	17,000	—
Gliadin	27,500	27,000
Hordein	27,500	—
Zein	40,000	—
Erythrocruorin (Arca)	—	33,500
Erythrocruorin (Chironomus)	—	31,500
Lactoglobulin	41,500	38,000
Pepsin	35,500	39,000
Insulin	41,000	35,000
Bence-Jones α	—	35,000
Bence-Jones β	37,000	—
Ovalbumin	44,000	40,500
Human tuberculous bacillus protein	32,000	—
Concanavalin B	42,000	—
Crotoxin	30,000	30,500
Haemoglobin (horse)	68,000	68,000
Haemoglobin (man)	63,000	—
Serum albumin (horse)	70,000	68,000
Yellow enzyme	82,000	78,000
Concanavalin A	96,000	—
Ribonuclease	13,000	13,000
Oxytocic-pressor hormone	30,000	—
Metakentrin	90,000	—

$3 \times 17,600$ and $4 \times 17,600$, and yellow enzyme falls between $4 \times 17,600$ and $5 \times 17,600$.

Now that some other low molecular weight proteins have been studied, the picture looks even worse for the reality of the unit. First of all, ribonuclease, with a molecular weight established between 13,000 and 14,000 by the two centrifugal methods and X-ray evidence, is 25 per cent smaller than the unit. Furthermore, to gliadin and hordein with molecular weights of 27,500 can be added the oxytocic-pressor hormone and also crystalline ficin with molecular weights of about 30,000; these four proteins are much smaller than $2 \times 17,600$.

It seems as if, the more proteins are studied, the less convincing the Svedberg unit becomes. I quote from an article by Pauling and

Niemann,[16] written at a time when the belief in the unit was widespread, "It seems to us, however, very unlikely that the existence of favored molecular weights (or residue numbers) of proteins is the result of greater thermodynamic stability of these molecules than of similar molecules which are somewhat smaller or larger, since there are no interatomic forces known which could effect this additional stabilization of molecules of certain sizes." This summarizes exactly our belief.

An interesting report concerning a newly investigated asymmetric protein has recently been published by Carter[17] from the Wisconsin laboratories. He found that nucleohistone from the calf thymus had f/f_0 equal to 2.6. As expected from such a value, the sedimentation constant was highly dependent on concentration, $s = 14.2 \times 10^{-13}$ for a 0.56 per cent solution and $s = 27.4 \times 10^{-13}$ for a 0.1 per cent solution. The limiting value was $s_{20}{}^0 = 31 \times 10^{-13}$. The diffusion coefficient was $D_{20} = 0.93 \times 10^{-7}$. It was observed that the diffusion curves were abnormal showing skewed displacement. Nevertheless the molecular weights arrived at by sedimentation, velocity, and diffusion on the one hand, and sedimentation equilibrium on the other were in excellent agreement with an average $M = 2{,}000{,}000$.

It should be noted that Lauffer estimated for tobacco mosaic virus, $f/f_0 = 2.5$, the same order of magnitude as that found for nucleohistone. But the variation in the constant of sedimentation for the same interval of concentration expressed in gm. per cent was only 17 per cent compared to nearly 100 per cent for nucleohistone. This difference comes probably from the fact that the change in concentration expressed in moles is very much smaller for tobacco mosaic virus than for nucleohistone.

DISSOCIATION OF MOLECULES

Lundgren and Williams[18] have drawn attention to the fact that $D = A\frac{f_0}{f}M^{-\frac{1}{3}}$, whereas $s = B\frac{f_0}{f}M^{-\frac{2}{3}}$, where A and B are constants depending on viscosity, specific volume of water, and density of solution. Hence, when a molecule dissociates, if the parts are more asymmetric than the whole, D may change very little because f_0/f decreases and $M^{-\frac{1}{3}}$ increases, whereas s will decrease because both f_0/f and $M^{-\frac{2}{3}}$ decrease. On the other hand, if the fragments are more symmetric than the original molecule, D will certainly increase. For example, if a

[16] **Pauling, L. & Niemann, C.** Jour. Amer. Chem. Soc. **61**: 1860. 1939.
[17] **Carter, R. O.** Jour. Amer. Chem. Soc. **63**: 1960. 1941.
[18] **Lundgren, H. P. & Williams, J. W.** Jour. Phys. Chem. **43**: 988. 1939.

molecule with an original asymmetry factor of $f/f_0 = 1.64$, corresponding to an oblong ellipsoid, with axis ratio, 1/12, according to the Perrin formula, and a diffusion constant, $D = A\frac{1}{1.64}M^{-\frac{1}{3}}$, is split along the long axis into two equal halves, one should expect a new frictional ratio, $f/f_0 = 2$, and the diffusion coefficient becomes $D = \frac{A}{2\sqrt[3]{0.5}}M^{-\frac{1}{3}} = \frac{A}{1.59}M^{-\frac{1}{3}}$. In other words, the variation in the diffusion constant would be negligible, whereas the ratio of the sedimentation would be about 4.3. If M remains constant with a decrease of f_0/f then both s and D will decrease. For example, phycocyan, with $M = 273{,}000$, dissociates into parts of 146,000, the sedimentation constant drops from 11.4 to 6.2×10^{-14} and the diffusion coefficient goes up from 4.05 to only 4.6×10^{-7}, the asymmetry factor being 1.2 for the whole and 1.35 for the parts. In the case of hemoglobin, the frictional ratio goes from 1.2 to 1.18 following splitting, which seems to indicate an increase of symmetry in the parts.

In conjunction with dissociation phenomena of proteins as observed with the ultracentrifuge, experiments carried out on the action of proteolytic enzymes on antibodies are worth mentioning. Many authors have used digestion with pepsin in order to purify diphtheria antitoxin according to the method of Parfentjev. Petermann and Pappenheimer,[19] as well as Tiselius and Dahl[20] submitted to pepsin digestion diphtheria antitoxin which behaved in the ultracentrifuge as a homogeneous protein with a molecular weight of 184,000 ($s_{20} = 7.2 \times 10^{-13}$). They obtained a new protein carrying the activity which, although not fully precipitated by toxin, was homogeneous in the centrifuge with $s_{20} = 5.7 \times 10^{-13}$, $D = 5.0 \times 10^{-7}$, $M = 113{,}000$. Tiselius and Dahl showed further that the split antitoxin was gradually digested by pepsin.

Northrop[21] purified antitoxin by trypsin treatment of the precipitate toxin-antitoxin at pH 3.7. He obtained a fraction which was 100 per cent precipitated by toxin, had a good solubility curve, and which he was able to crystallize. We examined[22] this fraction in the ultracentrifuge. There was only one homogeneous component with $s_{20}{}^0 = 5.65 \times 10^{-13}$, $D_{20}{}^0 = 5.76 \times 10^{-7}$, $M = 90{,}500$, and $f/f_0 = 1.23$.

It is interesting to note that the new antitoxin unit obtained by pepsin is probably very similar if not the same as that obtained by trypsin digestion. Petermann and Pappenheimer[23] have recently shown that

[19] **Petermann, M. L. & Pappenheimer, A. M., Jr.** Jour. Phys. Chem. **45**: 1. 1941.
[20] **Tiselius, A. & Dahl, O.** Ark. Kem. Mineral. o. Geol. **14B** No. 31: 1. 1941.
[21] **Northrop, J. H.** Jour. Gen. Physiol. **25**: 465. 1941–42.
[22] **Rothen, A.** Jour. Gen. Physiol. **25**: 487. 1941–42.
[23] **Petermann, M. L. & Pappenheimer, A. M., Jr.** Science **93**: 458. 1941.

similarly, antipneumococcus antibodies submitted to pepsin digestion were split and that the active portion was about of the same size ($s = 5.2 \times 10^{-13}$) as that found for antitoxin. All of this new information about the size of antibodies is interesting since for a time it was thought that animals could be divided into two groups with respect to the size of the antibodies produced. It seems now as if the active unit is considerably smaller but linked to different amounts of inert proteins according to the species of animal, the bonds being broken by pepsin or trypsin digestion.

To end this review on proteins as seen from the ultracentrifuge angle I should like to discuss some experiments bearing on the problems of denaturation. Since Svedberg's book, some progress has been made along this line and we know a little more than that "the processes of denaturation lead to polydispersity in the protein solution."

Lundgren[24] made an extensive study of the action of papain on thyroglobulin. He found first that under appropriate conditions a more slowly sedimenting protein, which he called α protein, was formed in a solution of originally homogeneous thyroglobulin. An equilibrium was finally established between the two forms. According to Lundgren, several other proteins behave in a similar fashion. He was able to show that it is the α form which is transformed into denatured protein, the denaturation being accomplished by heat or papain action. He made the curious observation that the denatured form sediments at the same rate as the original native protein in the absence of salt and appears to be heterogeneous in the presence of salt. It might very well be that the process of denaturation of a large molecule such as thyroglobulin proceeds along a different path from that followed by a smaller molecule like egg albumin.

In the case of egg albumin, Mirsky,[25] by titrating the SH groups liberated, has brought some convincing evidence that denaturation by urea is an unfolding process. If complete denaturation is accomplished by strong solutions of urea we found by sedimentation and diffusion experiments that the molecule has roughly the same molecular weight but that the asymmetry factor has become very much larger ($f/f_0 \backsimeq 2.2$) indicating complete unfolding. If the solution is then dialyzed, the molecules refold, as judged by titration and sedimentation, but the refolding happens in an apparently random way; the system is polydisperse and aggregation has occured. According to this view it is the refolding into the

[24] **Lundgren, H. P.** Jour. Biol. Chem. **138**: 293. 1941.
[25] **Mirsky, A. E.** Jour. Gen. Physiol. **24**: 709. 1940-41.

original or nearly original pattern which makes a so-called reversible denaturation possible.

It seems that a very slight change in the medium into which the unfolded molecule is dissolved may have some important effect on the way the refolding occurs. When egg albumin is heat-denatured with salt, refolding occurs in a random way with the appearance of large aggregates as often observed. In collaboration with Dr. K. Landsteiner we found that if the heat-denaturation is accomplished in the complete absence of salt the refolding occurs in a definite way, the material is homogeneous and the sedimentation constant is twice that found for the native molecule ($s_{20} = 7.0 \times 10^{-13}$, determined with 1 per cent salt added after cooling).

On the other hand, if heat denaturation is accomplished in the presence of only 0.2 per cent NaCl, refolding occurs also in a definite way; the material is homogeneous but the sedimentation constant is 5 times that of native egg albumin ($s_{20} = 17 \times 10^{-13}$ determined with 1 per cent NaCl added after cooling).

These results are striking inasmuch as they show the great importance of the presence of small amounts of electolytes for the orientation of the refolding process.

THE FUTURE OF THE ULTRACENTRIFUGE

Where lies the future of the centrifuge as a tool for the study of proteins? We have seen already that improvements could still be made in the direction of better control of the temperature. Another improvement would be to increase the sensitivity of the optical method to make possible the study of systems at very low concentration in proteins. In the case of biologically active substances, the concentration of the active material is very often so small that it is impossible to detect optically its sedimentary boundary. Refractive methods as they are used now could not be increased 10 times without difficulty. We should then try more sensitive arrangements. I think interferometric methods could be adapted for the ultracentrifuge and I believe Professor Beams has made some investigations in that direction. It would be a welcome improvement if we could narrow down the dangerous passage in extrapolating to zero concentration. Another improvement as mentioned above would be to calculate molecular weights by experiment of sedimentation equilibrium in nature but long before the equilibrium is reached. The integration of Dr. Archibald seems very promising and I am sure his theoretical results could well be used in this particular field of protein chemistry.

THE EFFECT OF CENTRIFUGAL FIELDS ON THE ELECTROMOTIVE FORCE OF GALVANIC CELLS

By D. A. MacInnes

From the Laboratories of The Rockefeller Institute for Medical Research, New York

The potentials of galvanic cells of the types

$$\text{Hg; HgCl, NaCl, HgCl; Hg} \qquad \text{(A)}$$

$$\text{(Pt); } I_2\text{, KI, } I_2\text{; (Pt)} \qquad \text{(B)}$$

would, under normal conditions, be expected to be zero. In both these cells two electrodes of the same form are in contact with a solution of uniform composition. If, however, the two electrodes of such a cell are at different heights in a gravitational field, or at different radii in a centrifugal field, small, but definite, potentials develop, as des Coudres[1] and Tolman[2] have shown.*

The equations relating the potential E of cells represented by types A and B to the other variables may be derived as follows. Under isothermal conditions the variation with a coordinate x of the chemical potential μ_i of a component, i, in solution will follow the differential expression:

$$\frac{d\mu_i}{dx} = \left(\frac{\partial \mu_i}{\partial x}\right)_{P,N} + \left(\frac{\partial \mu_i}{\partial P}\right)_{N,x} \frac{dP}{dx} + \left(\frac{\partial \mu_i}{\partial N_i}\right)_{P,x} \frac{dN_i}{dx} \qquad (1)$$

in which N_i is the mol fraction of the component i, and P is the pressure. The first term on the right hand side of equation (1) is given by

$$\left(\frac{\partial \mu_i}{\partial x}\right)_{P,N} = M_i f \qquad (2)$$

in which f is the force (gravitational or centrifugal) acting on one gram, and M_i is the molecular mass of the substance i. The term in equation (1) involving the pressure P may be put into more convenient form from the following considerations. The total Gibbs free energy Z of a system is given by the equation

$$dZ = -sdT + V\,dP + \mu_A dn_A + \mu_B dn_B \ldots + \mu_i dn_i \qquad (3)$$

in which s, T and V are the entropy, the temperature and volume, and μ_A, $\mu_B \ldots \mu_i$, n_A, $n_B \ldots n_i \ldots$ are the chemical potentials and the number of

[1] **des Coudres, T.** Ann. Phys. **49**: 284. 1893; **55**: 213. 1895; **57**: 232. 1896.
[2] **Tolman, R. C.** Proc. Amer. Acad. **46**: 109. 1910; Jour. Amer. Chem. Soc. **33**: 121. 1911.
* Since the conference at which this paper was presented, Grinnell and Koenig (**Grinnell, S. W., & Koenig, F. O.** Jour. Amer. Chem. Soc. **64**: 682. 1942) have published an important paper on the effect of differing heights of electrodes on the potential of a cell of type B.

mols of the substances indicated by the subscripts. By cross differentiation we have

$$\frac{\partial \mu_i}{\partial P} = \frac{\partial V}{\partial n_i} = \overline{V}_i \tag{4}$$

in which $\overline{V}_i$ is the partial molal volume of the constituent i. The gradient dP/dx is given by $-\rho f$ in which ρ is the density of the solution and f is, again, the force per unit mass. Thus we have from equations (1), (2) and (4)

$$\frac{d\mu_i}{dx} = (M_i - \overline{V}_i\rho)f + \frac{\partial \mu_i}{\partial N_i}\frac{\partial N_i}{\partial x}. \tag{5}$$

If the solution is allowed to come into equilibrium under conditions of constant force and pressure gradients the last term on the right hand side of equations (1) and (5) will acquire such a value that $d\mu_i/dx$ will become zero. However, in the experiments to be described below, the composition of the solutions involved remains constant throughout the cell, so that this term drops out and the gradients of chemical potential $d\mu_i/dx$ have finite values given by

$$\frac{d\mu_i}{dx} = (M_i - \overline{V}_i\rho)f. \tag{6}$$

In a gravitational field equation (6) takes the form

$$\frac{d\mu_i}{dh} = g(M_i - \overline{V}_i\rho), \tag{7}$$

in which h is the height and g is the gravitational constant. In a centrifugal field it becomes

$$-\frac{d\mu_i}{dr} = 4\pi^2 n^2 r(M_i - \overline{V}_i\rho) \tag{8}$$

in which r is the radius and n is the number of rotations per second. On integrating this equation between the radii, r_1 and r_2, we have

$$\Delta\mu_i = 2\pi^2 n^2(r_2^2 - r_1^2)\,(M_i - \overline{V}_i\rho) \tag{9}$$

The operation of the cell

$$\underset{r_1 \quad \rightarrow \quad r_2}{\text{(Pt); I}_2,\ \text{KI},\ \text{I}_2\text{; (Pt)}} \tag{C}$$

(in which the electrodes are at the radii, r_1 and r_2) per faraday of current passing in the direction indicated is as follows: (a) the transport of the Hittorf transference number, t_K, of equivalents of KI, from the region of the electrode at r_1 to that of r_2, and (b) the formation of an equivalent

of dissolved iodine in the region of r_1 and its disappearance from the electrode region r_2 by means of the electrochemical reactions

$$\text{I}^- = 1/2\ \text{I}_2 + e^- \quad \text{and} \quad 1/2\ \text{I}_2 + e^- = \text{I}^-$$

Since the change ΔZ of Gibbs' free energy for the process of the cell is equal to the algebraic sum of the changes of the chemical potentials during the process we have

$$-\Delta Z = E\,\mathbf{F} = t_K\Delta\mu_{KI} - \Delta\mu_I, \tag{10}$$

in which $\mathbf{F}$ is the faraday. With equation (8) this yields

$$E\,\mathbf{F} = 2\pi^2 n^2(r_2^2 - r_1^2)\,[t_K\,(M_{KI} - \overline{V}_{KI}\rho) - (M_I - \overline{V}_I\rho)]. \tag{11}$$

For very large speeds of rotation it would be necessary to consider the variation of the partial molal volumes $\overline{V}_i$ and the density ρ with the centrifugal force, but this is outside the limit of error of the work to be described below.* The experiments were essentially a continuation of the work of Tolman, with, however, the very considerable benefit of the advance of technology in the lapse of over thirty years. Due to the war emergency it has been found necessary to discontinue the research, we hope, temporarily. The results so far obtained are therefore put on record in this paper.

The apparatus, which is possibly nearer like that of des Coudres than that of Tolman, but differs considerably from both, is shown diagrammatically in FIGURE 1 (a) and (b). In that figure, (a) is a horizontal section, and (b) is a vertical section through the rotor, R, which consists of a magnesium alloy disk 23 cm. in diameter and 4½ cm. high. The rotor is suspended and turned by the shaft, A, which was driven, in the experiments to be described, by a direct current motor, through a belt and cone pulleys. This arrangement, with the addition of a rheostat, yielded speeds of rotation from about 750 to 5000 r.p.m. (The support and an improved drive will be described in a later publication.) Through the rotor is bored a 22 mm. hole into which the cell D and the counterpoise K are inserted. The galvanic cell D, the potential of which is to be determined, consists of a glass vial on the bottom of which is sealed a flat disk platinum electrode E' and at the neck is sealed a ring electrode E. Connections to these electrodes are made with platinum wires passing through the glass wall of the cell.

An important part of the apparatus is the commutator C. This consists of a pool of mercury into which is plunged a stiff wire, n, and above it an annular ring of mercury which makes connection with a hollow

* A more elaborate derivation, for the case of the variation of the electromotive force with height, is given by Koenig and Grinnell (**Koenig, F. O., & Grinnell, S. W.** Jour. Phys. Chem. **44**: 463. 1940).

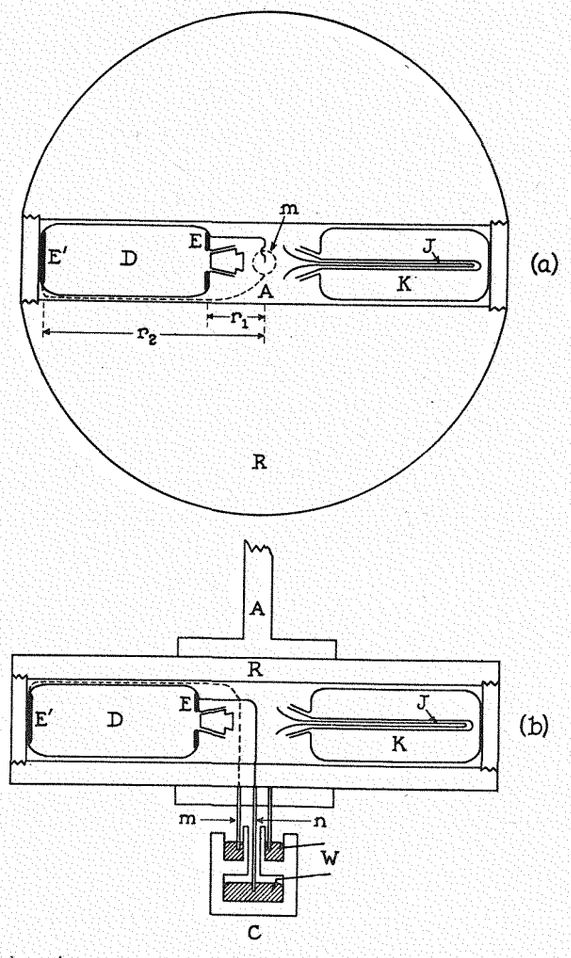

FIGURE 1. Schematic representation of centrifuge rotor *R*, cell *D*, counterpoise *K*, and commutator *C*. (a) Horizontal section. (b) Vertical section.

cylinder, *m*. The electrodes of the cell, *D*, are connected to *m* and *n* as shown. Dipping into the pool and ring or mercury are wires, *W*, which lead to the potentiometer. Up to speeds of 6,500 r.p.m. (the highest yet used in this connection), this commutator does not develop potentials over 0.1 microvolt. The speeds were measured with a Strobotac, with frequent calibrations.

In making measurements it was found that it was necessary to fill the

cell *D* completely since the presence of even a very small air bubble led to large and erratic potentials. It was also found that grease interfered with the measurements. The ungreased stopper was therefore placed into the full cell and the excess solution wiped away. The junction between the cell and stopper was then sealed quickly with hot paraffin. This operation was carried out in a constant temperature room, and contact with the hands was avoided, since expansions and contractions of the cell electrolyte resulted in air bubbles.

The measurements, so far, have been on the system:

$$(Pt);\ I_2\ (0.01\ M),\ KI\ (0.1\ M),\ I_2\ (0.01\ M);\ (Pt). \qquad (D)$$

At rest, this cell should have, as mentioned above, a potential of zero. When the electrodes were new this was far from being the case, since readings as high as 100 microvolts were observed. However, these potentials disappeared if the centrifuge were run at slow speeds, since even gentle vibration helps to bring the two electrodes to the same potential. Electrodes that had been some time in use gave initial potentials of only one or two microvolts.*

Beans and Hammett[3] and others have shown that platinum tends to absorb materials, chiefly of acid nature, which it slowly yields to solutions with which it is in contact. Vibration apparently tends to remove such contaminated layers of solution from the immediate region of the electrode. In all cases in which a bubble was absent from the cell the final potential was zero within one microvolt after a series of readings made first on rising and then on descending speeds of rotation.

A fairly typical set of measurements is plotted in FIGURE 2 in which the ordinates are potentials in microvolts and abscissae are to the squares of the rotational speeds, the highest value corresponding to 5,000 r.p.m. If equation (9) is valid this plot should be a straight line. As can be seen in the figure this is true for the data taken for the increasing speeds, as indicated by the arrow, but that there are deviations from this line as the measurements progressed and as the speed was decreased. In some cases the departure from linearity occurred at lower speeds than that represented in the figure.

It appeared probable that these observed deviations are due to a rise of temperature during the measurements. To test this assumption a copper-constantan thermojunction, *J*, was placed as shown in the

* Tolman[2] found large zero and residual potentials in all of his experiments. These were sometimes as high as 500 microvolts. These potentials had to be ignored if his results were to be interpreted in accord with theory. The explanation appears to be that the zero potentials largely disappeared as soon as the vibrations of the centrifuge started. Some of the zero potential was undoubtedly due to the fact that he included a bubble of air in his cell "to allow for temperature expansion and to allow for stirring of the solution."

[3] **Beans, H. T. & Hammett, L. P.** Jour. Amer. Chem. Soc. **47**: 1215. 1925.

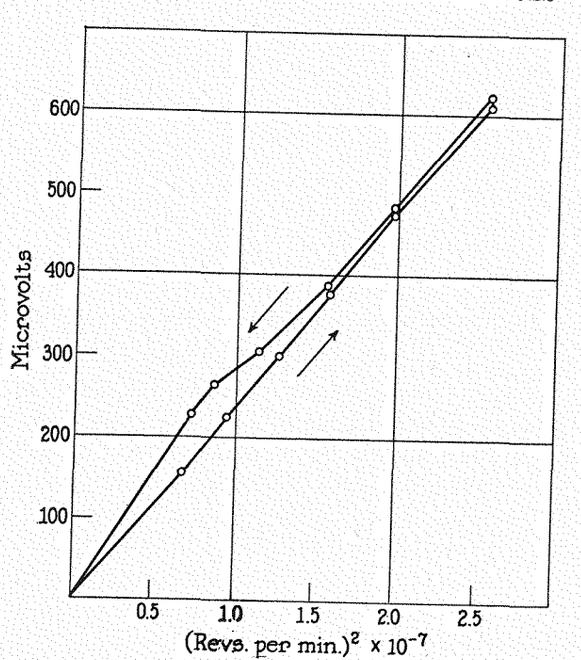

FIGURE 2. Electromotive force measurements during a typical determination.

counterpoise K of FIGURE 1, with a constantan wire running to the needle n of the commutator C, and a wire of that composition was placed in the lower mercury cup, which in turn connected with another junction in an ice bath. The extra copper-mercury and constantan-mercury junctions thus introduced into the circuit should cancel out, as they are at the same temperature. The potential obtained from this combination is a measure of the temperature of the interior of the counterpoise K, and thus, very closely, of the cell, D. The results obtained during such a series of measurements, occupying a period of time (one and one half hours) approximately equal to that used in obtaining the data plotted in FIGURE 2, are given also as a function of the square of the speed, in FIGURE 3. It will be seen that the temperature remained constant at the lower increasing speeds and then took a sharp rise at about 4,000 r.p.m. and reached its highest value at 5,000 r.p.m. On slowly reducing the speed the temperature rose slightly, and showed a slight decrease as the lower speeds were approached. (As a result of this observation the newly designed apparatus is fitted with a second commutator connecting permanently with the thermojunction in the counterpoise. By this

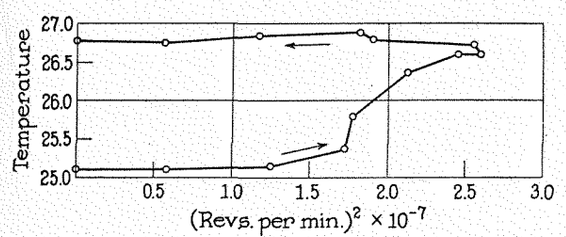

FIGURE 3. Temperature variation during a typical determination.

means it will be possible to measure, or control, the temperature, at the same time that the e.m.f. determinations are made.) Temperature variation is evidently an important, but not necessarily the only, cause for deviations such as are shown in FIGURE 2.

Measurements were made, using the apparatus shown in FIGURE 1, with two cells having the radii, r_1 and r_2, in centimeters, shown in the following tabulation:

	r_2	r_1	$(r_2^2 - r_1^2)$
Cell 1	10.23	2.08	100.32
Cell 2	10.29	1.45	103.75

The straight line portions of the data obtained with the two cells show considerable deviation from each other when plotted as in FIGURE 2, as would be expected. However, according to equation (11), the quotient, $E/(r_2^2 - r_1^2)$, should be independent of the dimensions of the cell and a linear function of the square of the rotational speed n, other variables, of course, being kept constant. That this is so, within the limits of accuracy of this work, is shown in FIGURE 4, where the linear portion of data obtained in determinations with cells 1 and 2 are plotted as described. It will be seen that the points lie on one line, in agreement with the theory.

On solving equation (11) for the transference number, t_K takes the form:

$$t_K = \frac{E\mathbf{F}/2\pi^2 n^2(r_2^2 - r_1^2) + M_I - \overline{V}_I\rho}{M_{KI} - \overline{V}_{KI}\rho}.$$

Using an average value of $E/n^2(r_2^2 - r_1^2)$, from the data plotted in FIGURE 4, of 0.825×10^{-10}, $\overline{V}_I = 30.90$ (for a 0.25M solution) from the work of Tolman,[2] $\overline{V}_{KI} = 47.18$ for 0.1 molal from the computations of Longsworth,[4] and a directly determined value, 1.0245, of the density of

[4] **Longsworth, L. G.** Jour. Amer. Chem. Soc. **57**: 1185. 1935.

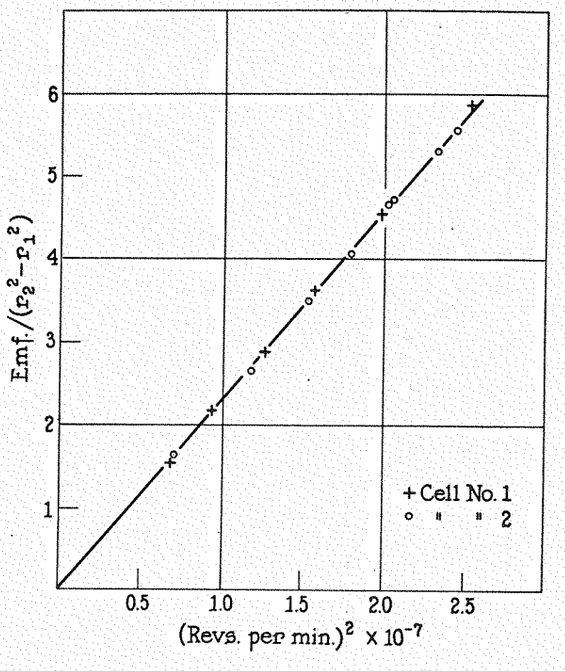

FIGURE 4. Comparison of electromotive force measurements obtained with cells of different dimensions.

the solution yields a value of the transference number, t_K, of 0.470. This agrees only approximately with the value 0.4883 obtained by Longsworth[4] for a 0.1 N solution at 25°C. The difference may be partly at least due to the use of an inappropriate value for $\overline{V}_I$.

It may be of service to compare the centrifugal method for determining transference numbers with the other available procedures, which are the Hittorf, the moving boundary, and the electromotive force methods. The Hittorf method requires electrodes that can carry considerable currents for long periods, utilizing only one electrochemical reaction, and careful provision must be made to avoid mixing of the solutions resulting from the electrolysis. Highly precise analytical data are also necessary since the method depends upon determining small differences between large quantities. The moving boundary method has yielded the most accurate data, but there appears to be a limit of concentration above which valid results cannot be obtained, and "indicator" solutions with the necessary properties do not always exist. The electromotive

force method requires two types of reversible electrodes, one each for the positive and negative ion constituents, and interpretation of the data to obtain transference numbers is frequently difficult. The centrifuge method, on the other hand, requires only one type of reversible electrode, which need not carry appreciable current. Such electrodes must, however, respond to very slight variations in the activities of the constituents of the electrochemical reaction occurring. The small potentials developed (of the order of one millivolt) must be measured with high precision. It seems possible that the centrifuge method will be useful in some cases in which the other methods are inapplicable, or function with difficulty. Examples are the determination of the transference numbers of weak acids and bases in aqueous solutions, and of electrolytes in non-aqueous solutions.

PUBLICATIONS

OF THE

NEW YORK ACADEMY OF SCIENCES

(LYCEUM OF NATURAL HISTORY, 1817–1876)

---

(1) The **Annals** (octavo series), established in 1823, contain the scientific contributions and reports of researches, together with the records of meetings of the Academy. The articles which comprise each volume are printed separately, each in its own cover, and are distributed immediately upon publication. The price of the separate articles depends upon their length and the number of illustrations, and may be ascertained upon application to the Executive Secretary of the Academy.

(2) The **Transactions**, reestablished as Series II in 1938, contain extended abstracts of papers presented before the regular sectional meetings of the Academy and other matters of general interest to Members, and are published monthly from November to June, inclusive.

Current numbers of the Annals and Transactions are sent free to all Members of the Academy. The Annals are sent to Honorary and Corresponding Members desiring them.

(3) The **Special Publications**, established in 1939, are issued at irregular intervals as cloth bound volumes. The price of each volume will be advertised at time of issue.

(4) The **Memoirs** (quarto series), established in 1895, are issued at irregular intervals. It is intended that each volume shall be devoted to monographs relating to some particular department of Science. Volume I, Part 1, is devoted to Astronomical Memoirs, Volume II to Zoölogical Memoirs. No more parts of the Memoirs have been published to date. The price is one dollar per part.

(5) The **Scientific Survey of Porto Rico and the Virgin Islands** (octavo series), established in 1919, gives the detailed reports of the anthropological, botanical, geological, paleontological, and zoölogical surveys of these islands.

Subscriptions and inquiries concerning current and back numbers of any of the publications of the Academy should be addressed to

EXECUTIVE SECRETARY

The New York Academy of Sciences

care of

The American Museum of Natural History,
New York, N. Y.

RUDISILL AND SMITH CO., LANCASTER, PA.

ANNALS OF THE NEW YORK ACADEMY OF SCIENCES
Volume XLIII, Art. 5. Pages 173–252

THE ULTRACENTRIFUGE

BY

D. A. MACINNES, W. J. ARCHIBALD, J. W. BEAMS, W. B. BRIDGMAN,
ALEXANDRE ROTHEN, AND J. W. WILLIAMS

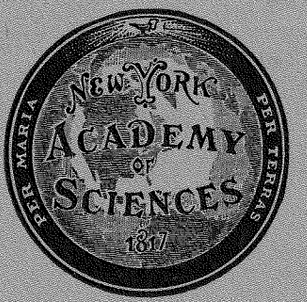

NEW YORK
PUBLISHED BY THE ACADEMY
October 6, 1942